YTTERBIUM DOPED ALL-FIBER INTEGRATED HIGH POWER LASER SYSTEMS AND THEIR APPLICATIONS

A THESIS

SUBMITTED TO THE DEPARTMENT OF PHYSICS

AND THE GRADUATE SCHOOL OF ENGINEERING AND SCIENCE

OF BILKENT UNIVERSITY

IN PARTIAL FULFILLMENT OF THE REQUIREMENTS

FOR THE DEGREE OF

MASTER OF SCIENCE

By

Saniye Sinem YILMAZ

July, 2013

I certify that I have read this thesis and that in my opinion it is fully adequate, in scope and in quality, as a thesis for the degree of Master of Science.

Assist. Prof. Dr. Fatih Ömer İlday (Advisor)

I certify that I have read this thesis and that in my opinion it is fully adequate, in scope and in quality, as a thesis for the degree of Master of Science.

Prof. Dr. Atilla Aydınlı

I certify that I have read this thesis and that in my opinion it is fully adequate, in scope and in quality, as a thesis for the degree of Master of Science.

Assoc. Prof. Dr. Hakan Altan

Approved for the Graduate School of Engineering and Science:

Prof. Dr. Levent Onural
Director of the Graduate School

ABSTRACT

YTTERBIUM DOPED ALL-FIBER INTEGRATED HIGH POWER LASER SYSTEMS AND THEIR APPLICATIONS

Saniye Sinem YILMAZ
M.S. in Physics
Supervisor: Assist. Prof. Dr. Fatih Ömer İlday
July, 2013

For the past decades, high-power laser technology has been developing rapidly all over the world. The scientific interest in fiber lasers stems from the rich nonlinear dynamics. Industrial interest is largely due to their practical advantages, such as high power levels, compact size, relatively low cost, excellent beam quality, over established laser technologies. As a result, fiber laser are highly sought after in applications including material processing, especially in high-precision micromachining with ultrafast pulses, medical applications and defence applications, especially for the high power and efficiency levels that fiber laser can offer. The advantage of fiber lasers for high powers is largely due to their geometry, which is a very long cylinder, with an extremely high surface to volume ratio, rendering heat transfer away from the active medium much easier. Fiber lasers diffraction-limited beam quality if operating in the fundamental fiber mode. Average output powers that can be extracted from singlemode fiber lasers can reach up to a few kilowatts without serious thermal problems due to the fiber structure. For many realworld applications, misalignment free operation is important and an all-fiber laser system offers this prospect, but to date, most of the published reports on high-power lasers utilise bulk optics components to couple light in and out of fibers, which detracts from some of the practical advantages of fiber lasers. Ytterbium doped fibers which are preferred as active media for high-power operation, as the technology behind it has led to the development of excellent components and the small quantum defect is extremely useful for high-power applications. Yb-doped continuous wave lasers practically can reach several kilowatt levels, yet the output power of Yb-doped picosecond and sub picosecond pulsed lasers with a small count of bulk optics in the cavity have been limited to several hundred watts.

In this thesis, we mainly focus on developing two high-power, robust, fiber-integrated lasers systems. The first system is a laser designed for continuous-wave (cw) operation, reaching up to 200 W level. The second system is a picosecond-pulsed system, delivering 100-W, few-ps pulses at 100 MHz repetition rate. The latter is built based on master oscillator power amplifier (MOPA) structure. The multi-stage amplifier of the pulsed system and resonator design for the continuous wave laser system are both based on the all-fiber designs which allow for robust operation and have been optimised through numerical simulations. We expect these systems to find widespread use in material processing applications.

Keywords: fiber laser, high power laser system, ablation, ytterbium doped fiber laser, ultrafast ablation .

ÖZET

İTERBİYUM KATKILI FİBERLE TÜMLEŞİK YÜKSEK GÜÇLÜ LAZER SİSTEMLERİ VE UYGULAMALARI

Saniye Sinem YILMAZ
FİZİK, Yüksek Lisans
Tez Yöneticisi: Yrd. Doç. Dr. Fatih Ömer İlday
Temmuz, 2013

Yüksek güçlü lazer teknolojisi, özellikle geçtiğimiz son bir kaç yıl içerisinde önemli bir gelişme göstermiştir. Bilimsel olarak fiber lazerlere ilgi, bu sistemlerin barındırdığı doğrusal olmayan dinamiklerden kaynaklanmaktadır. Endüstriyel alanda ise fiber lazerler, dayanıklıkları, esneklikleri, ucuz üretimleri ve sağladıkları yüksek ışın kalitesi nedeniyle tercih edilen lazer sistemlerinden birisidir. Bunun sonucunda fiber lazerler, malzeme işleme gibi bir çok uygulama alannda, sundukları yüksek güç ve verimlilikleri sayesinde aranılan sistemlerden olmuştur. Yüksek güç uygulamalarnda fiber lazerlerin; fiberin geometrisinden kaynaklı yüksek yüzey alanına bağlı hacim oranına sahip olması ile sistem içerisinde oluşan ısıyı hızlı bir şekilde dışarıya atması, bu sistemlere avantaj kazandırmaktadır. Fiber lazerlerde tek-modlu operasyonlarında, kırınım limitine yakın ışın elde edilir. Fiber lazerler; fiberin yapısından kaynaklı, çıkış güçleri bakımından teorik olarak herhangi bir termal sorun yaşamadan kilowatt seviyelerine ulaşabilmeleri tahmin edilmektedir. Endüstriyel alanlardaki uygulamalarda ince-ayar gerektirmezlik büyük önem taşımaktadır ve tümüyle fiberle tümleşik lazer sistemleri bu koşulu sağlamaktadır ama yayınlanan bir çok yüksek güçü fiber lazer makalelerinde, ışığın fiber içerisine gönderimi ve alımı için çeşitli fiberle tümleşik olmayan optik malzemeler kullanılmıştır. Bu durum fiber lazerlerin sağladığı avantajalardan bir kısmını engeller. Fiber lazerlerde yüksek güçlü çalışmalarda genel olarak ytterbium katkılı fiberler aktif ortam olarak kullanılır. Ytterbium kendi yapısından dolayı yüksek kazanç ve verimlilik ile birlikte; düşük kuantumsal kusurlar ve diğer aktif ortamlara göre düşük termal etkiler yaratır. Yb katkılı sürekli dalga fiber lazer sistemleri bir kaç kilowatt çıkış güçlerine ulaşmaktadr, ancak lazer sistemi atımlardan oluşuyorsa bu çıkış güçleri bir kaç yüz watt civarında olmaktadır.

Bu tezde genel olarak yüksek güçlü, dış etkilere dayanıklı, tamamen fiberle tümleşik lazer sistemleri üzerinde durulmaktadır. Birinci olarak, 200 W fiberle

tümleşik sürekli dalga fiber lazer sistemini geliştirilmiştir. İkinci olarak ise 100 W, 100 MHz, bir kaç pikosaniye atım uzunluğuna sahip fiber lazer sistemi geliştirilmiştir. Bu sistem MOPA yapısına bağlı olarak yapılmıştır. Salıngaç kısmında üretilen bir kaç pikosaniye atım genişliğine sahip atımlar, daha sonra üç aşamadan oluşan yükselteç kısmına gönderilir. Atımlı sistemin yükselteç kısmı ile sürekli dalga lazer sistemi tamamen fiberle tümleşik bir yapıya sahiptirler. Bu üretilen sistemlerin ileride malzeme işleme alanında geniş bir kullanm çerçevesine sahip olmasını beklemekteyiz.

Anahtar sözcükler: fiber lazer, yüksek güçlü lazer sistemi, ytterbium katkılı fiber lazer, yüksek hızlı ablasyon.

Acknowledgement

I would like to thank my advisor D. F. Ömer İlday for his invaluable support and guidance during my study. I am further indebted to Dr. Parviz Elahi for his mentorship throughtout my thesis work. I would like to acknowledge support by all the other members of Ultrafast Optics & Lasers Laboratory (UFOLAB) for their support and friendship. Our industrial partners, Koray Eken, Yiğit Ozan Aydın, Emre Yağcı from FiberLAST, Inc. made important contributions especially in the improvement of the robustness and reaching the highest power levels.

This thesis was partially supported by SAN-TEZ under grant 00255.STZ.2008-1.

Contents

List of Figures

List of Tables

Chapter 1

Introduction

1.1 Fiber Lasers

The word of laser is an acronym for light amplification stimulated emission of radiation. Stimulated emission is a fundamental concept in the basic understanding of laser action and first it was theorized by Albert Einstein in 1917 which makes possible to build lasers in theoretically. In 1958, Charles Townes and Arthur Schawlow theorized and published papers about a visible light laser, an invention that would use infrared and/or visible spectrum light. In 1960 Theodore Maiman invented the ruby laser and it was the first functioning laser in the world [1]. At the same time Gordon Gould published the term of Laser for the first time in the paper [2]. He dictated some possible application areas of lasers in his paper such as spectroscopy, ladar and interferometry. In 1962 first laser diode device was demonstrated by Robert N. Hall which was made from gallium arsenide and it emitted the light at 850 nm wavelength. Since the early period of laser history, laser research has produced a variety of improved and specialized laser types based on different performance goals such as maximum average output power, maximum peak power, maximum pulse energy and new wavelength band.

There are numerous types of lasers, which have developed over the past 50 years for scientific investigations as well as those for applications such as medical commercial and industrial uses. Although there are a wide variety of lasers, the basic working principle is the same for all laser systems. Lasers consist of a gain medium, a mechanism to supply energy to it and something to provide optical feedback. The gain medium is a material with properties that allow the light to amplify by stimulated emission. For the gain medium to amplify light, it needs to be supplied with energy which is called pumping. This energy is supplied as an electrical current or as light at different wavelength. Optical cavity is used as a feedback mechanism by the most of the lasers. A pair of mirrors is replaced on either end of the gain medium. Light reflects back and forth between mirrors, passing through the gain medium and being amplified each time. One of the mirrors is partially reflected and used as an output coupler. Laser types can be categorized in two ways. A laser can be classified as operating in either continuous or pulsed mode, depending on whether the power output is continuous over time or whether its output takes the form of pulses of light or can be categorized by the type of lasing medium.

Gas lasers are one of the laser types and low density gaseous materials are used as gain media. Gas lasers can be made from neutral atoms, ions or molecules for producing the laser light such as Helium, Neon, Argon, Carbon dioxide. Different gaseous material emits different wavelengths which varies from 193 nm (excimer laser) to 10.7 μm (Carbon dioxide laser). Basic working principle of gas lasers is based on resonant cavity. After building the resonant cavity with gaseous material as gain media, pumping the system is made by discharging the electrodes which are connected to gas medium. Inside of the cavity, electrical energy is converted to laser light. A most common gas laser is He-Ne laser which contains He atoms for collisional excitation of Ne. They are low power lasers and used for alignment purposes, holography, interferometry etc. Commercial carbon dioxide lasers can emit hundreds of watts as output power in a single spatial mode and this property gives carbon dioxide lasers to focusing their light into tiny spot size. They are pumped with RF discharge pumped and they can operate pulsed or continuous wave. The power conversion efficiency of carbon dioxide lasers are generally

higher than 10 % [3]. It is used very commonly for hardcore materials processing like cutting and welding.

Solid state lasers use high density solid media as active laser materials. Ions are introduced as an impurity into host materials, which can be crystalline or glass. Rare-earth or transition metals are preferred for gain medium. Host materials include crystals like sapphire (Al_2O_3), YAG ($Y_3Al_5O_{12}$) as well as glasses from silicate (SiO_2). Glasses as host material can be easier to fabricate, but crystlas have better thermal properties. Neodymium is the most common dopant in solid state cyrstals such as Nd:YVO4, (Neodymium yttrium ortovanadate) Nd:YLF (neodymium yttrium fluoride) and Nd:YAG(Neodymium yttrium aluminium garnet). Operating wavelength is 1064 nm. Nd:YAG is the most common solid state laser and it has widely usage. Especially they are used for metal cutting, welding and marking due to their high power outputs. The output of Nd:YAG lasers can be up to kW levels. Solid state lasers can operate either pulsed and continuous. Glass doped with Nd can support short pulse applications such as $\approx$ 100 fs duration. Nd:Glass is used for ultra short pulse, high energy, low repetition rate applications. Generally efficiency of solid state lasers are not high. Because of this reason thermal limitation occurs from unconverted pump power. This unconverted pump power manifests itself as heat. Nevertheless thermal limitations can overcome by changing the geometry of gain medium with smallest thickness. This method allows more thermal gradient in the material. Thin disk lasers are built based on this method and they can reach kilowatt output levels [4].

Chemical lasers obtains their energy from the chemical reactions inside of the system. With the continuous wave laser light they can reach megawatt output power. Wavelength of chemical lasers can vary from 1300 nm to 4200 nm. Hydrogen fluoride is the common one of this type of lasers and megawatt levels can be obtained with this lasers. Generally Hydrogen fluoride laser is used for laser weaponry because of their high level output power. Additionally they are common for cutting and drilling process.

Fiber lasers represent the latest generation of laser technology, which is distinguished from all the previous generations by being much more practical, as well as by its potential for generating high optical powers. Fiber lasers are a special type of solid-state lasers which are meant to be lasers with optical fibers as gain medium. Distinction between fiber lasers and all the other types of lasers originates in the fact that light in fiber laser cavities is guided and controlled by optical fibers. This feature enables a previously unprecedented degree of control over the light in a laser medium, which allows for the design of very efficient, robust, compact and reliable laser system.

Fiber lasers are the another candidate for high power laser systems because of high pump conversion to signal efficiency, stability and reliability. The geometric structure of fiber is also available for high power applications. Due to the fiber geometry, surface area to volume ratio becomes higher and excessive heat can be dissipated easier than other types of lasers. As a result, development of fiber laser technology is currently occuring, with a dramatic increase in the power levels into the few kW range and development will continue towards even higher optical powers ranging from a few kW to tens of kW, as required by a variety of emerging scientific, industrial, and defense needs. By recent developments, with fiber lasers 10 kW output power can be obtained with diffraction limited beam quality [5].

1.2 Fiber Laser Systems

Fiber optics which is used in modern technology is simple and relatively old technology. In the early 1840s, guiding of a light by refraction was demonstrated by Daniel Colladon and Jacques Babinet which makes fiber technology possible. First optical fibers which is based on total internal reflection principle were fabricated in the early 1920s [6]. However those fibers were sensitive to glass-air interface to environment effects. After development of cladding fibers [7], sensitivity of the glass-air interface to environment effects was reduced.

High-fiber losses prevented the building of long distance communication lines. Invention of low loss silica fibers with high purity were effective for reducing the losses less than 20 dB/km [8]. Modern optical fibers are typically made of very high-purity glass through vapor-phase deposition process, which minimize impurities, especially transition metal ions, to achieve very low transmission loss. The intrinsic loss of between 1 and 2 μm which is relevant wavelength range for most of fiber lasers, is at most a few dB/km. Modern optical fibers have losses below 0.2 dB/km which is obtained at a wavelength of 1.55 μm which is negligible in a fiber laser of a few meters distance. Modern telecommunication systems are based on this wavelength because of low loss in a long distance.

The basic structure of optical fibers is shown in Fig 1.1. They are used for transmitting light from one end to other end of fiber. Light propagates in the core based on total internal reflection principle while some part of the light penetrates into the cladding. Fused silica glass is used for the core of the fiber and its refractive index is represented with n_1. The core of the fiber is surrounded with cladding part and this part is also made from silica. Refractive index of the cladding is slightly lower than the refractive index of the core part which is represented with n_2. An acyrylic coating with higher refractive index is typically used both to protect the glass surface and to strip away any unwanted light propagation in the cladding glass.

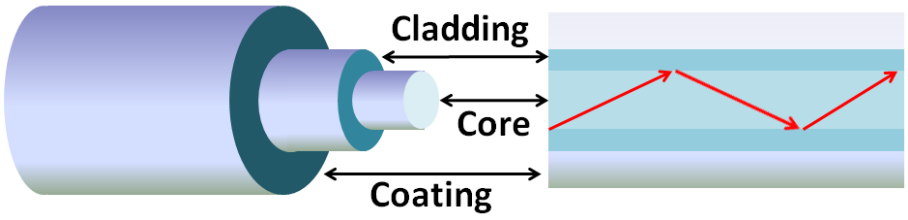

Figure 1.1: Basic structure of optical fiber and light propagation inside of the optical fiber.

Working principle of the optical fibers is based on the total internal reflection of light inside the fiber. Light propagates the core of the fiber and cladding part prevents escaping the light outside of the fiber. For the calculations generally

fibers are considered step-index which the refractive index is constant within the fiber core. Based on two different parameters of the fiber structure, numerical aperture (NA) which is a sine of the acceptance angle of fiber can be calculated.

$$NA = \sqrt{(n_1^2 - n_2^2)} \tag{1.1}$$

Another important parameter of fiber is V number which is also called as normalized frequency. V number determines the number of modes of the step-index fibers.

$$V = \frac{2\pi}{\lambda}\alpha NA \tag{1.2}$$

α is the radius of the fiber core and λ is the operated wavelength. If V number is less than 2.405 then the fiber supports only one mode (single mode fibers). The number of guided modes can be approximately calculated from given large V values by equation 1.3:

$$M \approx \frac{4}{\pi^2}V^2 \tag{1.3}$$

Due to technological transition, optical fibers became much more accessible for use in research laboratories and even industrial environments, thus accelerating the development of fiber laser technology. Nonlinear phenomena began to show itself as the intense light was forced to travel in the small core of fiber for long distances during the improvement of revolutionized the telecommunication industry. Raman and Brillouin scattering were observed in the 1970s [9, 10]. Interplay between the nonlinearity and dispersion causes soliton-like pulses and in 1973 were first suggested and experimentally observed in 1980 [11, 12]. Fiber amplifiers studies started with fiber laser development, since the laser requires a gain medium inside of the cavity. Fiber laser amplifiers started to emerge after 1980s. Fiber amplifiers were limited brightness of solid state diodes, which was hard to couple more than ≈ 1 W of pump power into core of fiber for amplifying the signal and this is the main factor for limiting output power of laser amplifiers.

This problem was solved by design of double clad fiber and now fiber lasers can go up to 10 kW in continuous wave operation [13].

1.3 Amplifier Systems

Optical amplifiers are that amplifies the input signal directly without converting any electrical signal or else. Optical amplifiers are just like a laser without feedback. Therefore, in the amplify systems cavities are not necessary. Under certain conditions, stimulated emission can provide a mechanism for optical amplification. An essential ingredient for achieving laser amplification is the presence of a great number of atoms in the upper state energy level than in the lower state energy level, which is nonequilibrium situation. An external energy source stimulates atoms in the ground state to transition to the excited state for creating a population inversion. This is a linear system that increases the amplitude of the input signal by a fixed factor which is called optical gain. Optical gain is the important parameter for these systems when the amplifier is pumped for obtaining population inversion. The gain of the ideal amplifier systems is the constant for all frequencies within the amplifier spectral bandwidth. In real amplifier systems typically has a gain that are functions of frequency. For large inputs the output signal saturates; the amplifier exhibits nonlinearity.

In general based on the energy levels of dopand, the pumping scheme can be classified in two groups like three-level and four-level scheme [14]. The main difference between three level and four level pumping scheme is that the ending energy state of ion after stimulated emission event. In three level system ion ends up in the ground state. On the other hand four-level system, it remains in an excited state. Obtaining desired gain and amplification for both schemes, getting a higher population inversion is the common point which means that higher ion density in the upper state depending on the pump power.

Amplifying process is based on three different types of photon-atom interaction. If the atom is in the lower energy level, the photon may be absorbed. If

it is in the upper energy level, a clone photon may be emitted by the process of stimulated emission. The third form of interaction is spontaneous emission which an atom in the upper energy level emits a photon independently of the presence of another photon. Figure 1.2 shows the scheme of these interactions for basic two level system.

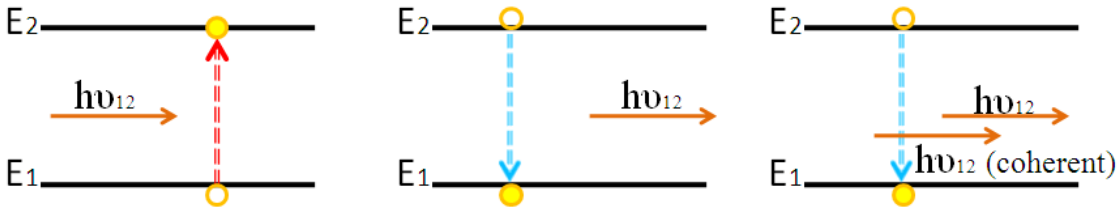

Figure 1.2: Photon-Atom Interaction: a) Absorption b) Spontaneous emission c) Stimulated emission

Depending on the energy levels of dopants, lasing scheme can be classified as three-level or four-level scheme. In either case, dopants absorb pump photons to reach an excitation stage and then relaxed rapidly into a lower energy excited state. 2- level system is the most basic lasing scheme for understanding dynamics of the amplification process. 3-level and 4-level systems are solved based on the same method of 2-level system. Fig 1.3 represents basic scheme of 3 level system. With the presence of amplifier radiation for 2-level systems transition between level 2 and level 1 stimulated emission takes a place with absorption. These processes can be characterized by the probability density where $W_i = \phi\sigma(\upsilon)$. The probability density for stimulated emission is the same as probability density for absorption. $\sigma(\upsilon)$ is the transition cross section at frequency υ and it can be identified as $\sigma(\upsilon) = \frac{\lambda^2}{8\pi t_{sp}} g(\upsilon)$. t_{sp} is the spontaneous lifetime and $g(\upsilon)$ is the normalized lineshape function. Based on these informations rate equations can be written,

$$\frac{dN_2}{dt} = R_2 - \frac{N_2}{\tau_2} - N_2 W_i + N_1 W_i \tag{1.4}$$

$$\frac{dN_1}{dt} = -R_1 - \frac{N_1}{\tau_1} + N_2 W_i - N_1 W_i + \frac{N_2}{\tau_{21}} \tag{1.5}$$

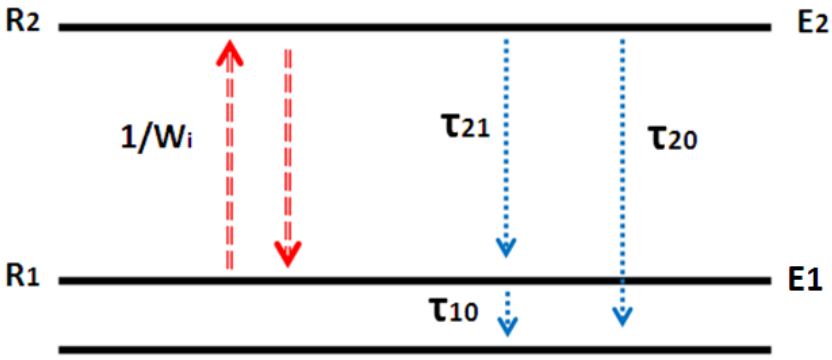

Figure 1.3: Illustration of three level lasing scheme

The population densities N_1 and N_2 are for the each energy levels 1 and 2 and they are determined by three process decay which is at rate $1/\tau_1$ and $1/\tau_2$, depumping and which is at R_1 and R_2 rate and finally absorption and stimulated emission at rate W_i rate. Figure 1.3 shows the basic scheme for energy levels of dopands and their transition rates during the lasing process with the presence of input signal.

In the steady state, namely, $\frac{dN_1}{dt} = \frac{dN_1}{dt} = 0$, the population difference in the presence of amplifier radiation (assuming absorption and emission cross section are equal $g_a(\upsilon) = g_e(\upsilon)$. This assumption is valid for both pump and signal) is;

$$N = N_2 - N_1 = \frac{N_0}{1 + \tau_s W_i}, \tag{1.6}$$

where N_0 is the population difference in the absence of amplifier radiation which is $N_0 = R_2\tau_2(1 - \tau_1/\tau_{21}) + R_1\tau_1$.
The characteristic time τ_s which may be called as saturation time constant is always positive because of $\tau_2 \leq \tau_{21}$.

$$\tau_s = \tau_2 + \tau_1(1 - \frac{\tau_2}{\tau_{21}}) \tag{1.7}$$

Gain coefficient of a laser medium $\gamma(\upsilon)$ depends on the population difference N which depends on the transition rate W_i and transition rate depends on the photon-flux density ϕ that is to be amplified. This situation is the basic of the

gain saturation. The gain coefficient represents the net gain in the photon-flux density per unit length of the medium. Equation 1.8 indicates the increament of optical intensity per unit volume in the direction of z [14].

$$I(z) = I(0)e^{\gamma(\upsilon)z} \tag{1.8}$$

Population difference becomes with the dependence of saturation photon-flux density $\phi_s(\upsilon)$

$$N = \frac{N_0}{1 + \phi/\phi_s(\upsilon)} \tag{1.9}$$

where $\phi_s = \tau_s\sigma(\upsilon)$. Then the gain coefficient becomes saturated gain coefficient where $\gamma(\upsilon) = N\sigma(\upsilon)$.

$$\gamma(\upsilon) = \frac{\gamma_0(\upsilon)}{1 + \phi/\phi_s(\upsilon)} \tag{1.10}$$

where $\gamma_0(\upsilon) = N_0\sigma(\upsilon)$. It is clear in equation 1.10 that, the gain coefficient decreases when the input photon-flux density increases which is known as gain saturation in amplifier systems.

Ytterbium ions are generally preferred gain media due to their efficiency, broad gain bandwidth and operational wavelength at 1060 nm. They are used for high power applications. Erbium-doped amplifiers have interest since 1985 [15]. However in some applications like telecommunications uses of erbium doped amplifiers have not been confined because obtaining high peak power has been gained interest. Also, operating wavelength of erbium doped lasers becomes unrelated for telecommunications. On the other hand, Ytterbium-doped amplifiers provides amplification to light over a very broad wavelength range. Yb-doped amplifiers also are appropriate candidates for high power applications. With their excellent power conversion efficiency and high doping levels are possible to lead to high gain in a short length. With the Yb-doped amplifiers, output power can be obtained more than 1 kW with diffraction limited beam [16, 17, 18].

Ytterbium-doped gain medium behaves like quasi-three level systems. Quasi-three level systems are like intermediate situation between levels three and four. In the quasi-three level systems, the lower laser level is so close to the ground state which appreciable population occurs in that level at the thermal equilibrium. For

the quasi three level systems spectral shape of the gain depends on the excitation level. Obtained laser wavelength may depend on the resonator losses which high losses require higher gain, consequently a shorter wavelength of maximum gain with small quantum defect [19]. With the increasing of the laser wavelength there is a transition between three level and four level characteristics. Ytterbium shows a three-level behaviour below 1040 nm wavelength and it shows strong three level behaviour around 1030 nm. With very small quantum defect, pronounced three-level behaviour is inevitable because this situation makes small energy space between the lower laser level and the ground state and thermal population of the lower laser level becomes significant.

Small quantum defect of ytterbium-doped amplifiers allows very high power efficiencies and also due to a small quantum defect thermal effects are reduced for high power applications. However quasi three level behavior of ytterbium-doped amplifiers may form some complications for small operating wavelengths. Ytterbium-doped amplifiers may be used for many applications including power amplification at special wavelength, free space laser communications and chirped-pulse amplification of ultra-short pulses [20, 21].

1.4 High Power Fiber Lasers and Challenges

Fiber lasers have significant practical advantages over bulk solid-state lasers or other types of lasers such as misalignment-free operation due to the guidance of the beam inside the fiber, also they have relatively simple thermal problems. Pump conversion efficiency and obtaining high beam quality are other important advantages of fiber lasers.

Therefore, high power fiber lasers are being used in the industry at a tremendous rate for the last five years all around the world and they are entering various new areas where they are replacing the previously used technologies. Low cost operation is the main reason for the replacement with previously used technology.

Continuous wave lasers are dominating the majority of industrial applications. Their output power levels vary from a few watts to several kW and they are generally used for cutting, drilling, welding processes. Figure 1.4 shows the progress of continuous wave fiber lasers with respect to last years [22]. For single stage continuous wave fiber laser world record output power is 10 kW [13]. Most of the highest power in continuous wave lasers are not all fiber design. Generally for continuous wave fiber laser systems, fiber is used for gain media and for the pumping process, bulk optics are used to launch pump light into the fiber. All-fiber integrated fiber laser design offers a simplicity and high reliability for real life applications rather than state of the art performance. 1 kW output power was reported for all fiber design in continuous wave laser [23] and to our best knowledge it is a world record for all-fiber design.

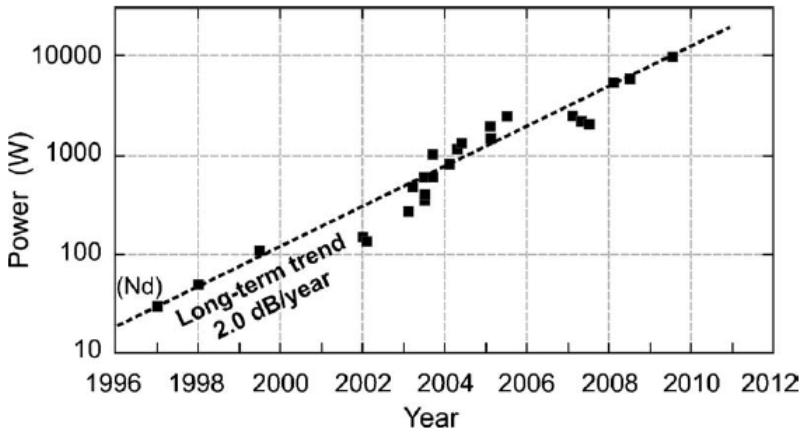

Figure 1.4: Increase of the output power level of continuous wave fiber lasers [14].

On the other hands pulsed fiber lasers are also used in the industry with relatively lower output power than continuous wave lasers. Nanosecond pulsed fiber lasers are adapted for material processing applications like continuous wave lasers. For the material processing both fiber laser systems have the same effects on the material. The work piece is simply heating to melting temperature with both laser systems. Average price level of a 1 kW continuous wave laser was around $100.000 and 20 W nanosecond pulsed laser was around $15.000. These results are important for the demands of pulsed laser systems. Pulsed lasers

provide high precision for material processing with lower cost than continuous wave lasers.

High power lasers with ultra-short pulses provides high precision material processing, so in recent years there is much scientific and limited industrial interest in the use of ultra-short lasers which are generating picosecond and femtosecond pulses. Especially in eye surgery, isolation in solar cells where precision is of utmost importance ultra-short lasers have great interest. Obtaining high average power is also important for ultra-short pulse lasers because of material properties. Transparent material like silica requires more energy for processing and high power lasers provides this demand.

For fiber lasers, highest output power for ultra-short lasers is reported as 830 W with femtosecond pulse duration [24]. Fiber is used as gain medium and bulk optics are used for pumping the gain medium and separating obtained signal light from pump light. Therefore, this system is not all-fiber integrated. In scientific research, most of high power fiber laser systems are not all-fiber integrated. All-fiber integrated systems have more advantages because light propagates inside of the fiber until the output of the laser. This design is safer and simpler for the user. Misalignment-free operation is also important for high power laser systems because in the infrared region eye can not see the laser light and for high power applications users must be more careful while system whose part contains bulk optics is working. Therefore, they are more preferred in industrial applications. However, all-fiber high power fiber laser systems have lower average power than bulk design. 157 W is the maximum output power for an ultra-short pulse duration and all fiber design [25].

Although high power laser systems have many advantages there are some limitations for reaching up to desired power levels especially for all-fiber design. Special components are required for high power parts of laser system especially for all-fiber designs and thermal problems are encountered because of pump conversion to signal light. For all-fiber laser design joint points of fibers should need special treatments. This section components of high power laser systems and limitation of high power laser systems are discussed.

1.4.1 Components of High Power Lasers

The first rare-earth doped fiber lasers have emerged as early as 1960 [26], while the first diode pump Er-doped fiber laser was demonstrated in 1968 at 1550nm center wavelength [27]. Due to technological limitations, those systems were operating at a few mW. The first fiber lasers and amplifiers were single mode devices in which both pump and signal propagates in small diameter fiber cores. However, in some applications those systems have not been confined because obtaining high peak power and high average power have been gained interest. Reaching up to high power levels was impossible with single mode devices. Therefore, new components and new technologies are required.

1.4.1.1 Double-Clad Fibers

Double-clad (DC) fibers are utilized for high power applications as they enable to pumping the system with relatively low brightness multimode diodes. In the recent days output power of pump diodes dramatically is increasing. For commercially 50 W fiber coupled pump diodes are available and they work without any heating or spectral problem for a long time. However for single mode single clad fibers it is impossible to couple that much power into the fiber. Therefore, new fiber geometry is needed for launching high power pump light into the fiber without any complications. Based on those demands double-clad fibers are produced. Their geometry contain two cladding part beside core part. These three layers have different refractive index. Laser light propagates inside of the core part as single mode and inside of the inner cladding which surround the core part pump light propagates. The numerical aperture of the core part is smaller than the inner cladding part and this allows the propagation of only one mode inside of the core. On the other hand inner cladding part has a bigger numerical aperture, so that it can support a large number of modes which allows the efficient launch of the output. Double clad fibers are made with different geometries for first cladding especially oblong geometry. Double clad fibers with oblong geometry yields better absorption efficiency [28], because with the circular cladding geometry there can be some guided modes of pump light whose intensity drops

to nearly zero at the center, which means some part of the pump light will not be absorbed by the active ions. By increasing the cladding diameter we can couple more pump power into the fiber. However this time we should increase the length of the gain fiber because the absorption coefficient of an active fiber is inversely proportional to cladding diameter and longer fiber brings the nonlinear effects which we do not want.

1.4.1.2 Pump Combiners

The easiest way to inject multimode pump light into the inner cladding of a double clad fiber is through the fiber end of the end pumping. This process can be done in two ways. First one is that two lenses are used for focusing pump light and coupling pump light into the DC fiber and also dichroic mirror can be used between two lenses to separate pump from signal light. The other way is using pump combiners. Most commercial high power lasers use fiber based combiners. The second way is the easiest and most usable way when compared to first one. Continuous wave fiber lasers with high power at multi kilowatt levels from single fiber have been demonstrated [29] with fiber based pump combiners. Also, pulsed fiber lasers can reach high power levels and high peak powers [25, 30], because those pump combiners enable multiple pump injections into the laser system. Pump combiners are main components for building all fiber laser structure.With the fiber bragg gratings, fiber coupled pump diodes and fiber coupled pump and signal combiners, all-fiber integrated architectures can be achieved. For a typical all-fiber laser system, there are a number of fused components which must be considered such as pump combiners, couplers, end-caps.

Pump combiners is to deliver multimode pump light into the first cladding of the fiber. For many applications including amplifiers, MOPA systems (Master Oscillator Power Amplifier), fiber based pump combiners are preferred. The most common fiber combiner is tapered fiber bundle which is based on the fiber end face pumping technique. In this type of combiners generally central input signal fiber is surrounded by several pump fibers and after organizing fibers whole bundle is tapered and cleaved around the taper waist. After those processes cleaved

end is spliced to the output fiber. Tapering process of fiber bundle changes the mode field diameter of the signal light, so some mechanical alignment and optical matching is needed during splicing between tapered fiber bundle and output fiber. With this structure, combiner loss their flexibility in the choice of input fibers and output fiber. Also, splicing disturbs the input signal and this can cause the degradation of beam quality. Therefore, splicing quality is important for this type of combiners. Pump combining into the fiber is another issue for these combiners. Coupling loss should be nearly zero which can be significant issue in very high power lasers. Otherwise there will be heating inside of the device.

1.4.1.3 Signal Combiners

As the demand for higher output power increase, the onset of nonlinear effects and fiber damages must be taken into account. Signal combining techniques can help overcoming these limitations since they allow the power scaling to the kilowatt range by merging the output of several hundred watts of few kilowatt fiber lasers into single large core delivery fiber [31, 32]. Signal combiners is to combine multiple fiber laser outputs. These can be either be incoherently or coherently combined. For the signal couplers, coupling characteristics of the input beams depend on the taper length, taper ratio, and the length of the straight section. Recently Coherent beam combining has great interest for both power and brightness scaling [33]. The goal of coherent beam combining is to combine high power laser beam so as to obtain single beam with high power and preserved beam quality.

1.4.2 Challenges

Even though in recent years the progress in the development of high power levels of fiber lasers have shown a remarkable increase, various kind of more or less severe limitations are now encountered, which are expected to slow this progress. Fiber laser systems have immune to effect of heat generation due to their special geometry. However, heat dissipiation per unit length has reached values of the

order of 100 W/m [34] in recent years, which causes significant heating for air-cooled systems and excessive heat generation causes thermal beam distortions and severe damages on the fiber laser system. Secondly, nonlinear effects are the main concerns in high power fiber laser systems especially in pulsed operations, coming before the thermal problems that comes from small mode size and large propagation length in nonlinear medium. Sticking to the all-fiber design, output power of fiber lasers is also limited by splicing qualities and making an extremely small loss splice is the key point in all-fiber design. This section will explain these difficulties that limit the laser from reaching higher power levels.

1.4.2.1 Thermal Effects

Thermal problems of lasers are known to be the prime limiting factor for the operation of high output power levels. High power fiber lasers have attracted considerable attention in industrial and military applications. Fiber geometry which is very long and thin cylinder with a very large surface to volume ratio allows for an exceptional capacity of heat dissipation and hence, reduction of thermal lensing effects. However thermal management is still one of the most important issues for reaching higher output powers for high power fiber lasers. In high power fiber lasers, components are subject to extremely high power density which can lead to major failure caused by the severe thermal effects. Therefore, excessive heat should be dissipated from the system for achieving high output powers. Two main points which are splice points and doped fiber, should be taken care of carefully. Also, low index polymer coatings of fibers are sensitive to high thermal load and it can be damaged when the temperature approaches approximately 200 degrees. Therefore, temperature of coating of fiber is needed to be controlled.

Ytterbium-doped media is preferred for high power laser operations because of a low quantum defect of ytterbium ions. Quantum defect is the energy difference between pump wavelength and signal wavelength. This energy difference turns into heat energy because of photon-phonon of host material interaction in the active media. Therefore, the small quantum defect makes ytterbium a prospective

for efficient lasers and power scaling. Their pump conversion efficiencies are at maximum 80% [35]. Nevertheless, some part of pump light is converted to heat energy and for kilowatt power levels heat generation becomes significant and catastrophic failure becomes inevitable unless some precautions are considered.

The easiest way to inject pump light into the fiber is through the fiber end of end pumping. Pump light is launched into the system from fiber tips. For end-pumping scheme, uneven temperature distribution is occurred because of non-uniform pump absorption in the fiber and an excessive heat generation is occurred near the fiber ends due to higher pump absorption. Using lower pump absorption could be the solution for reducing the heat generation. This solution reduces the temperature of the system based on the simulations, but it also reduces the efficiency of the system [36]. Most of the pump absorptions are near the fiber ends which causes major heat dissipations at those points. For continuous wave fiber lasers reducing the absorption coefficient and increasing the active fiber length could be solution but this reduces the efficiency of the system. For pulsed fiber lasers increasing the fiber length may ignite the unwanted nonlinear effects inside the laser system. Therefore, for high power pulsed systems shorter fiber length is usually preferred and other techniques should be considered for reducing the heat dissipations which we will discuss in detail in chapter 3.

Building all-fiber integrated high power laser design is the main purpose of this thesis. We use fusion splice for connecting the fiber based components of laser systems. Fiber connection between passive fiber where pump light is launched and active fiber is the most important part for all-fiber design in high power operations. Heat generation occurs at the tip of active fibers because of higher pump absorption coefficient. Therefore, this splice point has significant importance for the system and it should be excellent for preventing any heat dissipations and damages because of losses and heat generation. Splicing process will be discussed next section and also subsections in chapter 2 and chapter 3 in detail.

Polymer coating is indispensable for handling of the fiber, has a low thermal stability and constitutes the limiting factor for heat load in the fiber. Due to quantum defect of active ions temperature is rising during the operation and polymer coating can be damaged. For long term stability of high power fiber laser, cooling is necessary for keeping the operating temperature of an active fiber.

1.4.2.2 Splicing

Splicing is the process by which a permanent low-loss, high strength, welded joint is formed between two fibers and ultimate goal of splicing is to create a joint with no optical loss yet that mechanical strength and long term reliability that matches the fiber itself. Achieving low-loss splices between different fiber types comprising such fiber devices poses technical challenging. For high power laser systems, splices between different component have a significant role because of the possible losses at those points and this situation limits the output of the laser.

Preparing fiber tips properly is the first step for fiber splicing. Fusion splicing always requires that the fiber tips exhibit smooth end face which is perpendicular to the fiber axis. After cleaving the fiber there may be some distortions on the end face of fibers. Those distortions are the one of the most common causes for geometric deformation in the resulting splice. Much of the variation in splice loss observed between different splices fabricated using the same splice parameters is due to variation in cleave quality.

After the splicing process some geometrical distortions may be encountered like air holes, bubbles and airlines because of various reasons . Dirt on the fiber tips can become trapped at the splice and forms bubbles or defects on the fiber can cause airli nes at splice joints. Bubbles, holes and airlines usually do not reduce the strength of a fusion splice. However, bubbles typically induce splice loss. Vertical airlines also do not reduce the strength of splice, but they result from refraction of light at the surface of the splice joint.

Figure 1.5: Bubbles and vertical airlines cause high splice loss. Airlines cause refraction of light at the splice joint.

Fig 2.11 shows the lower splice quality. Splice joint can refract the light so as to give the appearance of either a bubble of vertical line at the exact site of the splice. Existence of bubbles and vertical lines at the splice joint indicate reduced strength and reliability [37].

Enhancing the splice quality may prevent damage which are caused by the combustion because of excess heat around splice points. Therefore, preparation of splice operation has significant role for high quality splice points. Cleaning and cleaving fiber tips properly may prevent most common distortions at the splice joint.

Proper fiber tip preparation for splicing is enough for reducing the splice loss if two same fibers are used. In this thesis, we use two different kinds fibers for splicing. One of the main splices is that splice between active fibers and passive fibers. Active fibers contains active ions inside of their core and due to active ions core of the active fiber behaves different from passive fiber during the splice operation. When an optical fiber is heated to high temperatures such as those encountered during fusion splicing, the active ions can diffuse through the glass material. Therefore, they are changing the optical and mechanical properties of the fiber which means that a core diameter of active fiber increases more than

passive fiber core diameter. At the end after fusion splicing we may encounter core mismatch because of different core diameters. In chapter 2, we will discuss the active fiber splice strategy in detail.

Another important splice for this thesis is that splicing between two different core/cladding size fibers. For this kind of splice, alignment of fibers become important for obtaining low loss splices. Therefore, we use active alignment for splicing. There are two types active alignment for splicing [37]. One is an image based active fiber alignment which controls fibers with positioners based on a digital image of the fiber tips obtained with microscope objective and digitizing camera. Another technique is transmitted-power based fiber alignment. This alignment technique contains optical light source and power meter. This optical light source is coupled into one of the fiber and with aid of power meter we measure the transmitted light from other fiber. Based on the transmitted light we make the alignment.

1.4.2.3 Nonlinear Effects

Nonlinear effects impose fundamental limitations on high power laser systems especially for pulsed systems because light is confined in the fiber core and propagates for a long distance in a nonlinear medium. When intense light propagates in silica, optical response of a material changes and nonlinear effect which is called Kerr effect instantaneously occurs in the medium. It is described as dependence of refractive index on the intensity of light. The strength of nonlinear effects can be represented as [38]

$$S_{NLE} = \int_0^L \frac{P_{peak}(z)}{A} dz, \tag{1.11}$$

where L represents the fiber length and P_{peak} represents the peak power at position z along the fiber and A is the in-core guided mode field area. In fibers, nonlinear effects occur due to either the intensity dependence of refractive index of the medium or inelastic scattering phenomenon. Due to the power dependence of refractive index, Kerr effect occurs. Kerr effect manifests itself in three different

effects based on the input signal such as self-phase modulation (SPM), cross-phase modulation (XPM) and four-wave mixing (FWM). At the higher intensity levels in the laser systems, this time inelastic scattering phenomenon starts to be observed such as stimulated Brillouin scattering (SBS) and stimulated Raman scattering (SRS). For inelastic scattering phenomenon, if the intensity of the incident light exceeds a threshold then the intensity of scattering light starts to grow exponentially.

SBS is related to the third order susceptibility $\chi^{(3)}$ and it can be effective at very low power if the conditions are suitable. Brillouin scattering consist of an inelastic energy exchange between incidents photons and phonons in the host material. Pump photon is annihilated to produce Stokes photon and acoustic phonon. The frequency difference between the incident and scattered photons is called Brillouin shift and it equals to $\upsilon = 2n\pi\upsilon_a/\lambda$. n represent the effective index of the fiber and λ is the wavelength of the incident photon. υ_a indicates the velocity of acoustic phonons. For silica this value equals to 10 GHz with a bandwidth of 10 MHz. This process is stimulated by the presence of the generated Strokes photons and acoustic phonons in the fiber. Estimation of the Brillouin threshold at critical pump power P_{cr} is;

$$\frac{g_B P_{cr} L_{eff}}{A_{eff}} \approx 21, \tag{1.12}$$

where g_B is the peak value of Brillouin gain which is equals to $g_B = 5 \times 10^{(-11)} m/W$ for optical fiber at 1555 μm. L_{eff} is the effective fiber length and A is the mode field area. For ultra-short pulse propagation, if a sufficiently broadband spectrum is used then SBS is not effective and can be safely ignored.

Stimulated Raman scattering (SRS) is the most important nonlinear effect which limits the performance of high power systems. Above some threshold value for SRS, in quantum mechanically pump photon is annihilated and a Stokes photon and optical phonon are generated. SRS are initiated at a threshold value. Equation below shows the approximation for threshold value of SRS,

$$P_{cr}^{SRS} \approx 16 \frac{A_{eff}}{g_R L_{eff}}. \tag{1.13}$$

Here, P_{cr}^{SRS} is the critical power for SRS and g_R is the peak Raman gain and it scales inversely with pump wavelength.

Stimulated Raman scattering and Stimulated Brillouin scattering are similar to each other. For both cases the incident photon with frequency w is annihilated and a photon with strokes frequency ($\omega_s = \omega - \omega_v$) is created. The difference between SRS and SBS is that generated phonons (acoustic) with SBS are coherent and give rise to macroscopic acoustic wave in the fiber, but during SRS phonons (optical) are incoherent and no macroscopic wave is generated. For ultra-short pulse propagation, if broadband spectrum is used then SBS is not effective and can be safely ignored. On the other hand SRS has a significant contribution on the propagation of ultrashort pulses and it can not be ignored during measurements.

Chapter 2

200 W All-Fiber Continuous Wave High Power Laser System

High power CW laser sources from a hundred of watts to several kilowatts are required for different industrial applications especially material processing such as cutting, welding of hard metals. Fiber lasers and amplifier systems are more preferable because of their high efficiency, stability and especially their nearly diffraction limited beam even in high power applications. Addition to the large surface area to volume ratio fiber lasers can dissipate heat faster, so controlling of operation temperature of laser system becomes easier than other types of lasers. The most powerful laser systems in the literature are the continuous wave systems and with the development of technology, 10 kW fiber laser has been built and it is the highest output power which was reported for single mode operation [13]. In despite of the all high power achievements, these fiber laser systems are not totally all-fiber integrated. For the majority of high power fiber lasers, active medium contains fiber and diode stacks are utilized with lots of optics for spatial beam combining and focusing pump light into fiber for pumping the system. Therefore, fiber lasers loss their flexibility and simplicity. All-fiber integrated laser design is an alternative approach for obtaining not only flexibility and simplicity but also high power output. All-fiber design is more compact for kilowatt fiber lasers and amplifiers comparing to other types of lasers. In this design, there are no diode

stacks and lenses. Those bulk optic components are replaced by fiber coupled diodes and multi-mode pump combiners (MPC) and dichroic mirrors are replaced by fiber Bragg gratings (FBG). However power level of all-fiber laser systems are below the free-space systems. Recently 1 kW all-fiber integrated laser system has been developed and it works on a single mode operation [23].

Advance of high power lasers contains three major technologies, such as high-quality active fibers, passive fiber components which can handle high power applications and bright pump diodes. Here, we report on the development of an Yb-doped large-core CW laser with 200 W output power, operating at a central wavelength of 1060 nm. To our best knowledge, this fiber laser system has the one of highest output power for all-fiber and non-commercial fiber laser system based on all-fiber design [23, 39, 40, 41]. The cavity is entirely fiber-integrated, including pump delivery, which renders the system misalignment free. The linear laser cavity comprises of a section of DC Yb-doped fiber, a high-reflector fiber-Bragg grating (FBG), a low-reflector FBG functioning as output coupler, a pump combiner with 19 pump ports, and up to 12 high-power (25 W) pump diodes. This output power is limited by the available pump power and splicing quality (fiber connection points). In this study, Emre Yağcı helped in the construction of the experimental setup and measurements.

2.1 Simulations

There are a large number of parameters that need to be optimized for high-power operation with high output coupling as well as well-suppressed amplified spontaneous emission (ASE) generation, length of the gain fiber, signal and pump absorption levels. To this end, a numerical model was developed, based on the well-known model in [42], to closely guide the selection of these parameters. The model was implemented in a MATLAB environment. For the simulation of realistic high power laser systems the Lorentzian gain model is not sufficient. Therefore, a new model was developed which uses the original absorption and emission cross-section of Yb in the gain fiber. In this model, rate equations were used for

calculating the upper and ground state population [42]. Simulation software is modelled as two level gain medium. After setting the initial values of a pump and signal powers at the entrance of the fiber, after that initial values are iterated throughout the gain fiber several times until a steady state is reached. Mathematically we can write the two coupled differential equations and solve them which are discussed in detail at appendix A and MATLAB code for this simulation is in appendix B.

After this point we investigated how the system parameters affect the output of the system. Therefore, we need some initial parameters for running the simulation. The gain fiber has a core diameter of 25μm, numerical aperture of 0.08, and a cladding diameter of 250μm. The pump combiner has with 19 pump ports. The high-reflector (reflectivity of 99%, centered at 1060 nm) fiber-Bragg grating (FBG) and another FBG with a low reflectivity of 7%, also centered at 1060 nm and with a bandwidth of 2 nm complete the cavity. Pumping is provided by up to 12 fiber-coupled, multimode (MM) diodes centered at around 976 nm. Each of the pump diodes provides up to approximately 24 W of power, corresponding to a total available pump power of 285 W. Given the rather narrow (a few nm) absorption band of Yb-doped fibers around 980 nm and the propensity of the diode wavelength to shift with temperature, it is important to characterize their performance. To this end, the optical power, central wavelength and optical bandwidth of the pump diodes were determined. Fig 2.1 shows the measured spectrum bandwidth, wavelength and power of diodes which are being used as initial parameters for simulation.

After obtaining the the important input parameters, various different arrengement were investigated. First, we investigated the type of FBGs which were used. In continuous wave operation, gain saturation reduces the gain for high input power. When input signal is so weak, gain saturation is not observed. Therefore, low-reflective FBGs affects the efficiency of the output power which is used 7% FBG in the current system. When the reflectivity is dropped 1%, energy of the intracavity it also decreases which this affects the pump absorption in the cavity inversely. On the other hand, when the reflectivity is increased to 50% then increments of the intracavity energy increases the total loss while dropping the

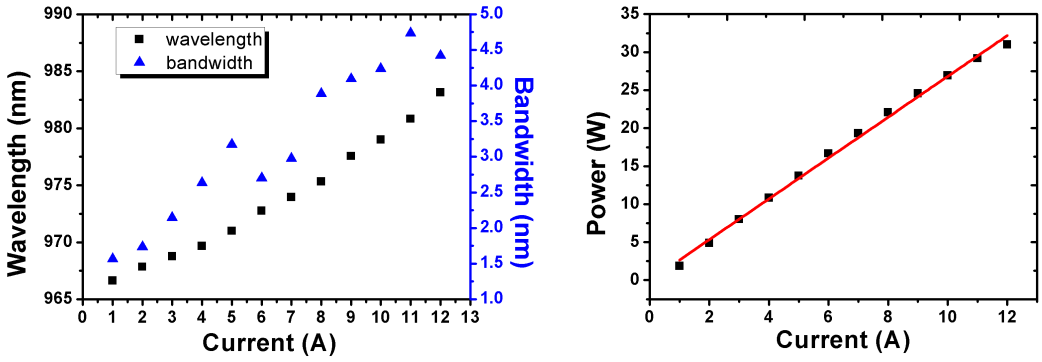

Figure 2.1: (a) Central wavelength and optical bandwidth of a typical diode as a function of the pump current. (b) Output power as a function of the pump current for a typical diode.

efficiency and output power. Fig 2.2 shows simulation results for two different FBG reflectivity. 99% FBG, length of the active fiber and pump power which is 300 W are same for both configuration, only reflectivity of low reflective FBG is changed. Green line indicates the pump absorption and black (dashed line) is for forward signal propagation. Pink (dotted line) is for backward signal propagation through the acitve fiber.

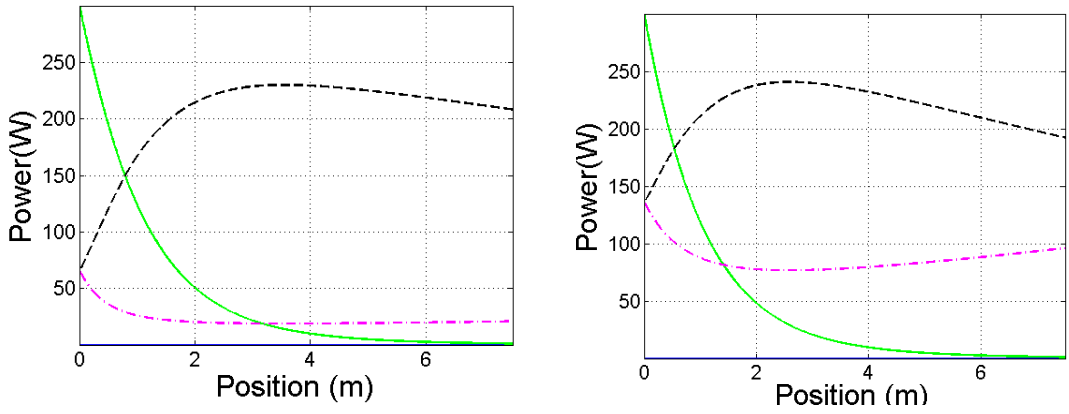

Figure 2.2: The effect of reflectivity ratio of the low reflective FBG (a) 1% reflectivity (b) 50 % reflectivty.

In Fig 2.3 shows the variation of the output power with respect to the reflectivity for 150 W launched pump power and 7.5 m active fiber length. As seen on the figure, obtained output power is expected to increase due to the decrease in reflectivity of FBG.

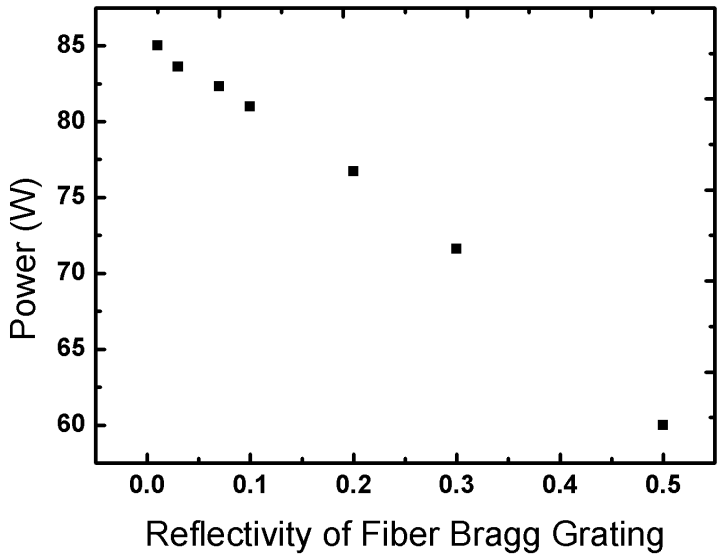

Figure 2.3: Variation of reflectivity of FBG and expected output power.

Figure 2.4 shows numerical calculations of the system. The launched pump light which is represented by green line is injected from the left-side of the active fiber. After launching the pump light into the system signal starts to propagate in the forward direction which is shown as black dashed line and it is reflected from FBG with 99% reflectivity. Reflected signal which is magenta and dash-dotted line, after reflecting FBG with 7% reflectivity turns back to the beginning of the fiber whereby, a cavity is formed and 93% percent of light is taken out as the output of the laser.

We investigated the effect of doping concentration on the fiber length. For high doping concentration, we expected to use a shorter fiber length or visa versa. Fig 2.4 shows the simulation results for different doping levels and fiber lengths for maximum output power. First figure has 2× higher doping concentration than

second figure. Therefore, fiber length is 2× shorter than low doping concentration fiber for obtaining maximum output power. Pump absorption of high doping concentration fiber is 2×faster than the low doped fiber. In Fig 2.4 (a) pump absorption is indicated with green solid line and is consumed approximately first 2 meters of the gain fiber. On the other hand Fig 2.4 (b) pump light is consumed approximately in the first 4 meters of the gain fiber. Obtained maximum output power is same for both case and is around 230 W. However fiber length is different for maximum output power.

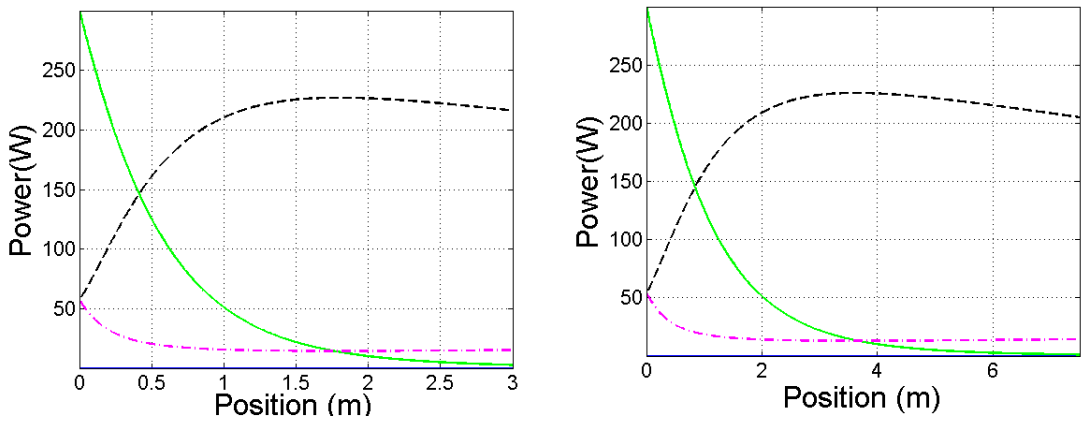

Figure 2.4: (a)Using high doped gain fiber. (b)Using low doped fiber.

Pump parameters also affect output parameters of this system such as pump power and pump wavelength. We simulated the effect of pump wavelength and pump power on the system. We set value of FBG to 7% and used low-doped concentration gain fiber at 7.5 meters like Fig 2.4(b). We found that fiber length is independent of pump power which can be seen in Fig 2.5(a) which launched pump power was 600 W. On the other hand, pump wavelength has a significant role in fiber length, because the narrow absorption peak of Yb-doped fibers is at 976 nm. When wavelength-shifted pump is used, then pump absorption drops and optimum fiber length increases as seen on the Fig 2.5(b).

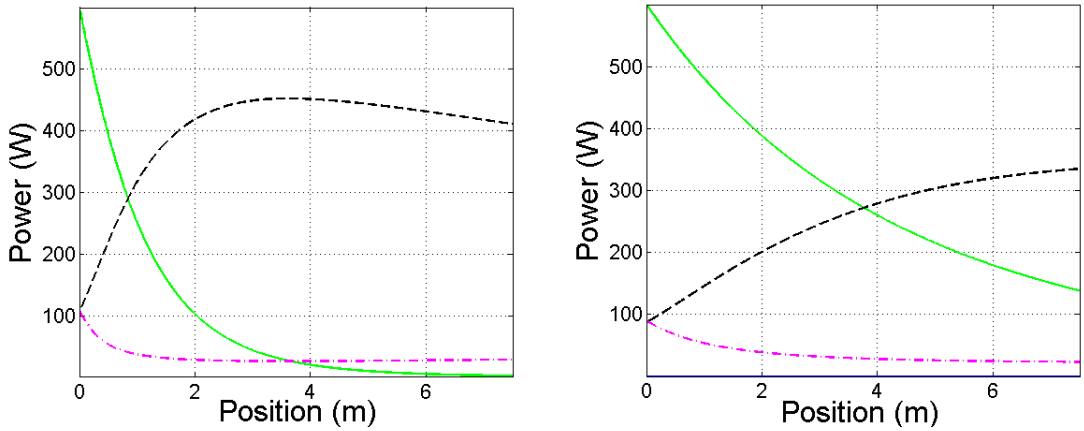

Figure 2.5: The effects of pump parameters. Numerically calculated pump (green, solid line), forward signal(black, dashed line), backward signal (magenta, dash-dotted line). (a) 600 W pump power is launched into the system at 975 nm wavelength. (b) 600 W pump power at 985 nm wavelength.

The numerical simulations indicate that about 200 W of intracavity power should be generated at the output coupler (Fig 2.4 (b)). Upon extraction of most of this power, the beam amplified back to about 30 W before reaching the high reflector, where the unabsorbed pump power is estimated to be also around 30 W. At ASE generation remains negligibly small under these conditions. The optical spectrum is expected to be centered at 1060 nm with a bandwidth of approximately 1-2 nm.

2.2 Experimental Results

The schematic of the experimental setup is shown in Fig 2.6. In this configuration there are two types of fibers. First one is the pump fibers which have 105 μm core diameter and 125 μm cladding diameter with 0.15 NA. The other fiber type is 25/250 DC fiber which has 25 μm core diameter and 250 μm cladding diameter. DC stands for "double-clad" fiber which brief information can be found in Chapter 1.2.2.

Numerical apertures of 25/250 DC fiber are 0.07 for the core and 0.46 for cladding. Numerical aperture also quantifies the strength of guidance and affects the number of modes which survive inside of the fiber [43]. Large mode area single mode fibers can have low numerical aperture below 0.06. Fibers which have numerical aperture values are around 0.3 is called multimode.

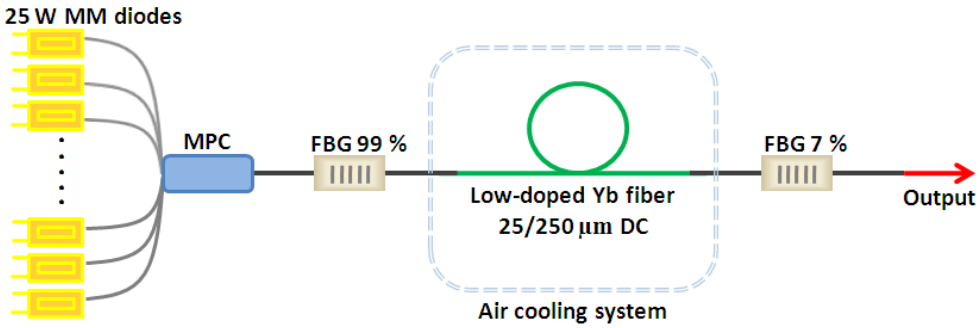

Figure 2.6: Schematic of the all-fiber CW fiber laser.

Active medium consists of 7.5 meter Yb-doped fiber (Liekki Yb700-25/250 DC) with the doping concentration approximately $5 \times 10^{25} m^{-3}$ which is based on simulation results. Length of active fiber is affected from doping concentration and shorter fiber length can be used for high doping concentration. However, a major heat dissipation can be occured due to high pump absorption coefficient at splice joint of high reflective FBG and gain fiber. Splice point can be burned unless the excessive heat is rolled out. Therefore, we can solve this problem in two ways. First one is dissipating the excessive heat with extra cooling system and the other one is reducing the heat generation by using low doping concentration fiber instead of high concentration one.

For pumping the system, 12 pieces 25 W capable pump diodes are used from Oclaro. They can supply 24 W output power at 10 A current and at 10A most of the diodes emits 976 nm wavelength light where Yb absorption is maximized. Fig 2.1 shows the characteristics of pump diodes which are used in laser.

Two FBGs are used in this system as dichroic mirrors which are produced as

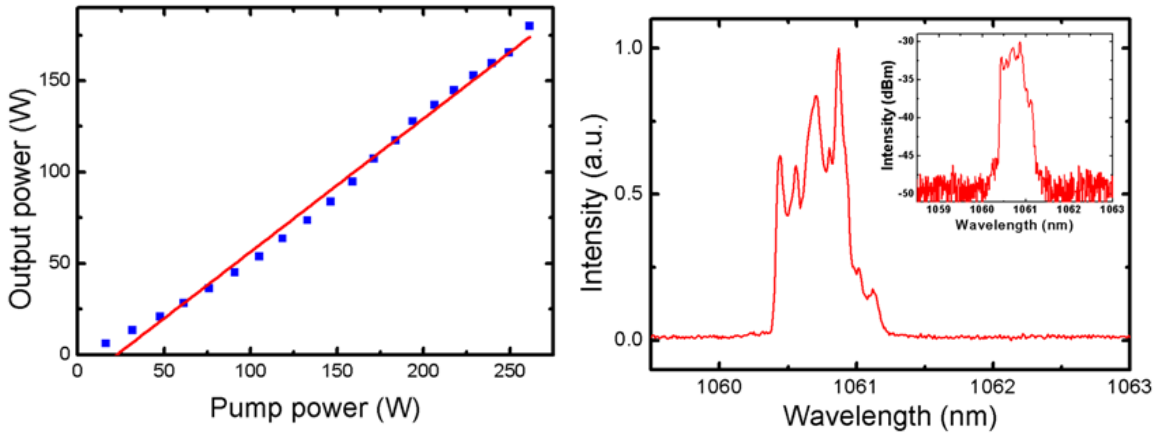

Figure 2.7: (a)Measured output power with respect launched pump power. (b)Output spectrum at the maximum output of 200 W.

a pair by nLight. One of them is highly reflected as 99% percent and the other one is partially reflected as 7%. Their reflectivity becomes maximum at 1060 nm wavelength with 0.3 nm bandwidth. Fig 2.7 shows the output of the system versus launched power with a slope efficiency 71% and the output spectrum is given at 200 W. As seen on the power scale there is no sign of saturation and the graph is fitted with linear line. This indicates that the system is pump power limited. While we were taking the measurement for the output power, power fluctuations at the few percent level were observed. Since the large mode area fiber is not strictly singlemode, higher-order spatial modes may be excited, leading to power fluctuations as a result of their beating. Another possible reason is thermal fluctuations associated with the narrow band FBG. Similar fluctuations are not uncommon and have been reported elsewhere [16].

2.3 Challenges

2.3.1 Thermal Effects

During lasing process, 285 W pump power is delivered through the system and most of the pump light is converted to signal light, yet because of the quantum defect, we can not achieve full conversion efficiency. With the existence of thermal effects physical properties of fiber can be changed, also beam quality of light can be affected. However, we can not prevent heat generation which occurs because of conversion efficiency of pump light along the active fiber. Therefore, thermal dissipation and the prevention of damage to optical components and fiber become the most important issue.

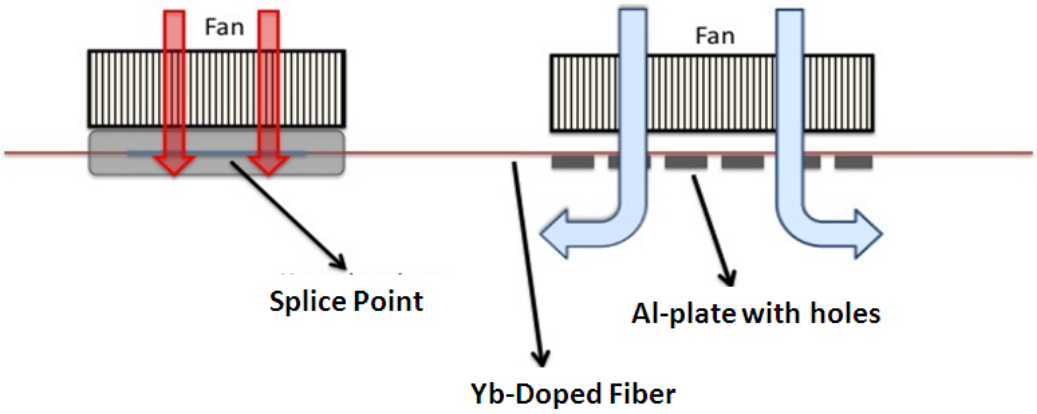

Figure 2.8: Design of the air cooling system.

Thermal management of splices in high power fiber lasers is also challenging issue, because the heat load of the active fiber is caused by pump loss absorption. Splice point between passive fiber and active fiber contributes to heating because of splice losses of pump light and pump absorption losses.

After the splicing process, we do not recoat that splice point with coating material because the polymer coating can not handle for high temperature due to its low thermal stability.

Air cooled approach have been opted for splice points and gain fiber. Fig 2.8 shows the design of the cooling system. There are two air fans in that design. One is for a cooling box which contains a splice point of FBG and gain fiber which is embedded into the thermal paste. The heat dissipates faster with thermal paste and air fan cools box of splice point. The other fan is top of the gain fiber and aluminum plate. There are holes in that plate for providing the air flow. With this method heat can easily dissipiate from the gain fiber.

2.3.2 Splices

Achieving low-loss splices between different fiber types comprising such fiber devices poses technical challenging. For high power laser systems, splices between different component have a significant role because of the possible losses at those points and this situation limits the output of the laser. Especially splice between highly reflected FBG and gain fiber is the most critical part in the system. Enhancing the splice quality may prevent damage which are caused by the combustion because of excessive heat generation around splice points and losses at the site of the splice.

Splicing process contains many parameters which affect the splice quality. The parameters of the fusion splicer should be well optimized for the fiber type. After cleaning and cleaving the fibers, fibers are put on the fiber positioners inside the splicer. Alignment is also important for obtaining low loss splice and slightly difficult because of hexagonal geometry of active fiber. Alignment operation is based on image-based fiber alignment. First, we align the claddings of fibers and after that core alignment is done for low loss signal transmission with fiber positioners. Electrodes of the splicer are the heat source of splicer. The heat source may be an electric arc which a resistively heated metal filament. This method is the most common splicing method to heat fiber tips. Electrodes heat

the fiber ends and cause them to fuse together. The splice heating power is often measured in units of mA but in our case we use resistively heated filament as a heat source whose heating power is measured in W.

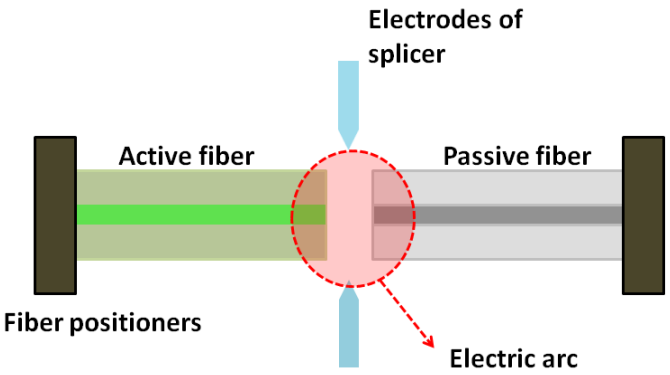

Figure 2.9: Schematic of splices process.

Splice duration is the amount of the time that the heat source is applied to the fiber and it is about second levels. The gap between the fiber tips is usually arranged around μm level at the beginning of the splice operation. After heating fiber tips this gap is reduced to zero by the hot push with fiber positioners. Fig 2.9 shows the schematic of splice operation of active fiber and passive fiber.

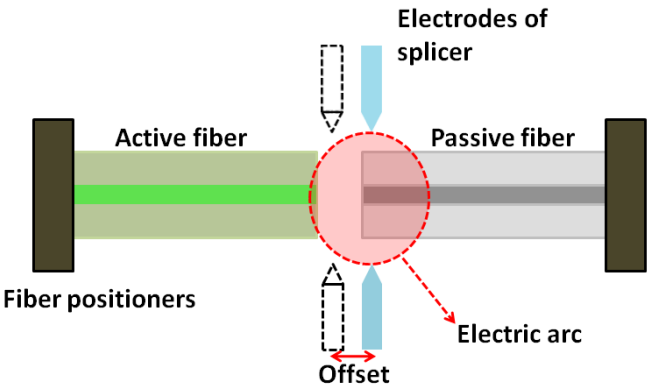

Figure 2.10: Schematic of splice process with offset to electrodes.

A splice of ytterbium-doped fiber is difficult to make with low-loss because of the mode field diameter and mode field shape mismatch. Also, dopand diffusion is

effective for splice loss. Heating treating splice between doped fiber and passive fiber causes the mode field diameter of doped fiber expands faster than mode field diameter of passive fiber. At the end we obtain splice with mismatched fiber core. Therefore, we can simply extend the splice heating time which is lifetime of electric arc or we can give offset to electrodes and make closer to passive fiber. Fig 2.10 shows the offset of the electrodes. We can prevent extra extension of active fiber core by giving less heat than passive fiber.

Offset distance and splice quality can be optimized with arranging the splice parameters such as arc time, arc power and push parameters. We can not use transmitted power method for splice quality. Measured power is not reliable at the end of active fiber after splicing operation because given light is absorbed by active ions of fiber. Therefore, we need to trust the image of splicer. Fig 2.11 shows the good quality splice. As seen on the figure, cores of fibers are well aligned and there is no bubble, airline or holes. There is no sign of fattened or tapered splice joint which they can be fixed by changing the arc power and hot push distance.

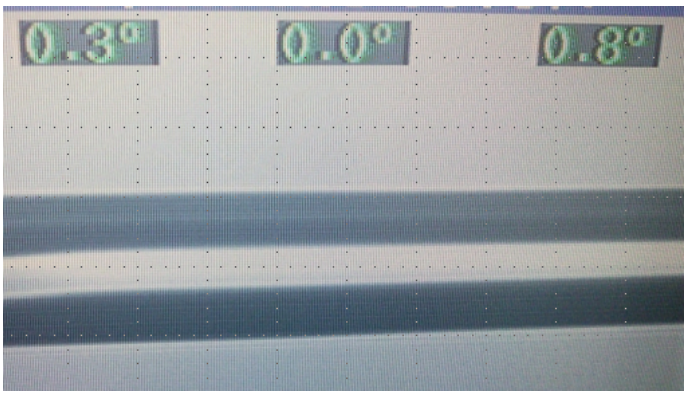

Figure 2.11: Image of high quality splice. Cleave angle of left fiber is 0.3^o and 0.8^o for right fiber. These angles are acceptable for high splice quality. There are no asymmetrically fattened or tapered splice between two fibers. There are no bubbles, airlines or holes at the splice joint.

2.4 Conclusion

As a result, all-fiber integrated CW laser has been built with 200 W of output power at 1060 nm wavelength. This continuous wave laser system is the one of the highest power all fiber integrated laser systems in the world. Measurement results shows that the only limitations for this system are both pump power and thermal loading. The slope efficiency of the system is 71% and appears not to show any sign of saturation. This efficiency is already close to similar systems using bulk optics for pump coupling [44]. Simulation software which is modeled the laser as 2-level system is useful for giving an idea about the effects of system parameters on the overall efficiency of the system. The air cooling design was presented, which should allow better control of thermal load on the laser. All-fiber integrated systems are more compact and flexible comparing to other types of lasers with the same power levels. We expect to achieve higher output power in the near future through more advanced fiber design, combined with more powerful pump sources. Exceeding power scaling beyond the kilowatt level in a single fiber configuration looks entirely feasible with all-fiber laser design.

Chapter 3

100-W 100-MHz Few Picosecond Pulse Generation From An All-Fiber Integrated Amplifier

In recent years, there is much scientific but limited industrial utilization of ultrafast fiber lasers, generating picosecond and femtosecond pulses, for material processing [24, 45, 46]. For high precision micromachining, pulsed laser deposition and surface texturing, pulsed lasers have a significant place because of their high peak powers despite the low average power. Apart from the peak power of the pulses, increasing the average power has great benefits with increasing the repetition rates for especially material processings.

High repetition rate and picosecond pulses can be easily obtained from mode-locked lasers and low repetition rate can be obtained on Q-switched or directly modulated diode lasers. In this work, we demonstrate the fiber integrated Yb-doped laser with few picosecond pulse duration and 100 MHz repetition rate. As an average output 100 W is measured with all-fiber integrated amplifier. This system is designed for high precision and high speed micromachining. Note that the most of the results which are presented in this chapter were published in [20] (copyright ©2012, Optics InfoBase).

3.1 Experimental Results

High power and high energy pulsed laser system are built based on MOPA (Master Oscillator Power Amplifier) configuration. This configuration is based on one oscillator part where low power pulses are formed and the amplifier part where peak power of the pulses is amplified. Our setup contains oscillator part and three stage amplifiers. For arranging the pulse duration, gratings part is included in this configuration. This system has been designed for making micromachining with high precision. Using ultra-short pulses, the ablation process can be easily controlled because material is removed in small quantities, thus assuring high processing accuracy and cleannes. The main obstacle to a wide spread of laser micromachining, despite their unique possibilities, is the fabrication efficiency. The way of increasing the efficiency of micromachining process is to increase the repetition rate and average power of laser system. Therefore, 100 MHz repetition rate has been chosen based on speed parameter and pulse duration should be smaller as possible as we can. Schematic of the experimental setup can be seen in Fig 3.1.

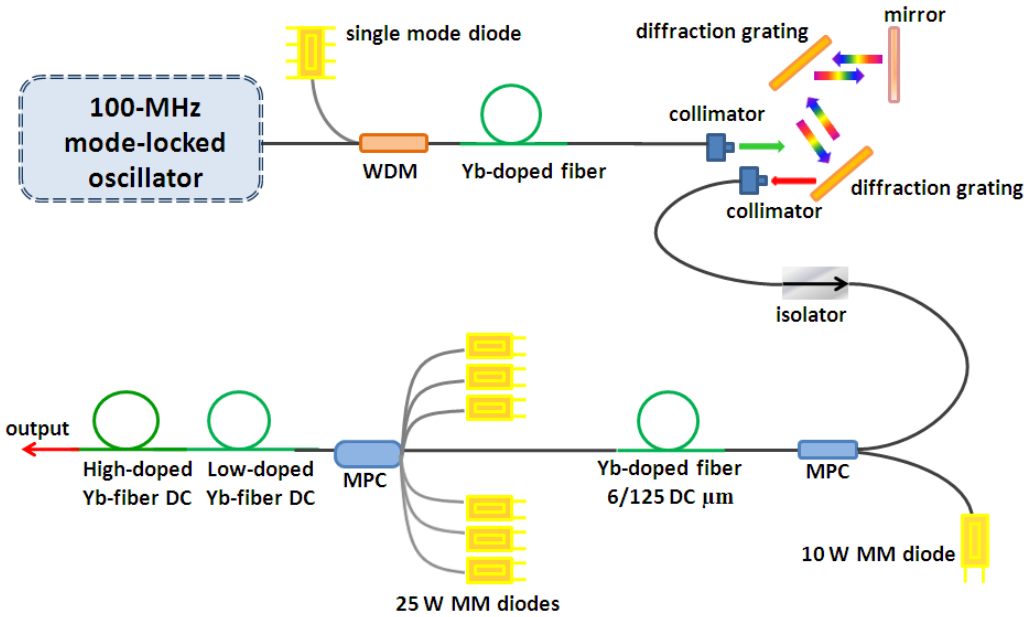

Figure 3.1: Schematic of the setup.

In this system, pulses are generated in oscillator part and 1.2 mW output power is obtained with a 100 MHz repetition rate. After oscillator, pulses are passing through the first amplifier part for increasing the average power to 100 mW and second amplifier comes after the first amplifier for increasing the average power up to 1.5 W. Last part is the high power amplifier and at the end of the system 100 W average output power is obtained. The amplifier comprises of three stages, which are all fiber integrated and delivering 13-ps pulses at 100-W. For high precision micromachining, pulse duration must be lower than a few picosecond. By placing a grating compressor after the first stage amplifier, negatively chirped pulses can be launched into the last two stages of amplification, which allows partial management of the interplay between the pulse chirp and self-phase modulation. We generated few picosecond pulses at 100 W average output power with this method.

3.1.1 Oscillator Part

We preferred all-normal dispersion mode-locked Yb-doped fiber oscillator as a seed. Several distinct mode-locked regimes can be utilized such as soliton like, stretched-pulse, similariton, and all-normal dispersion. Among these, the ANDi laser does not require the use of diffraction gratings and has the potential for all fiber integration. Owing to its simplicity and robustness, we have adapted an ANDi laser as seed source. The fundamental repetition rate of the oscillator is 100 MHz. For calculating the repetition rate of the oscillator equation 3.1 is used. f_R is the repetition rate of the system and n is the refractive index of the fiber which is 1.5. L_{fiber} and L_{air} are the lengths of the light path. L_{fiber} is equal to 184 cm for the this configuration and L_{air} is equal to 23 cm inside the oscillator. With this parameters repetition rate coincides to 100 MHz.

$$f_R = \frac{300MHz}{nL_{fiber} + L_{air}} \tag{3.1}$$

Fig 3.2 illustrates the experimental configuration of oscillator part. Active fiber is pumped with single mode pump diode at 976 nm wavelength and pump is

launched through a 976/1030 nm wavelength-division multiplexed (WDM) coupler. Yb-doped fiber is used for gain media and it has 500 dB/m gain at 976 nm with 6/125 core/cladding diameters. Based on the simulations the all-normal dispersion comprises of a 60 cm long single mode Yb-doped fiber.

Free space section of the oscillator is approximately 23 cm and contains quarter and half waveplates for polarization control and a bulk isolator for polarization selectivity and to force unidirectional operation. An interference filter with 10 nm bandwidth is placed. The filter's influence in the time domain is to remove the temporal wings of the pulse, and assist the saturable absorber.

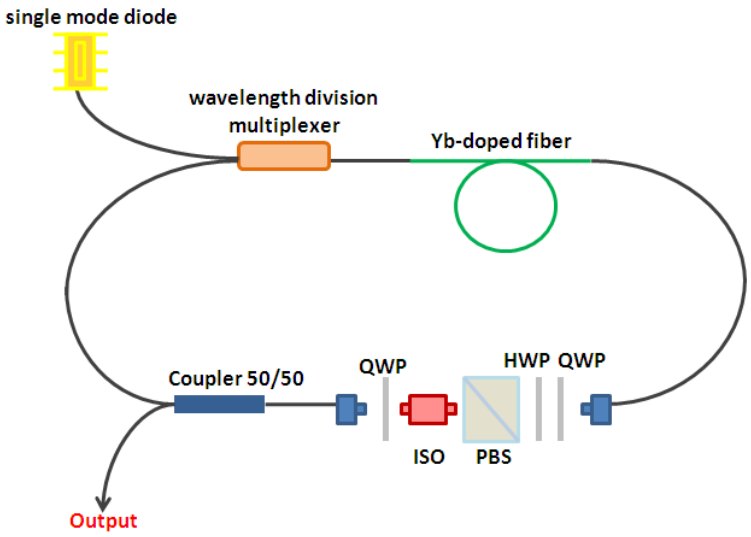

Figure 3.2: Schematic of oscillator works at 100 MHz.

Saturable absorption is implemented through nonlinear polarisation evolution (NPE), which is achieved using a half wave plate, a pair of quarter wave plates and a polarized beam splitter (PBS). We can use rejected light from the polarized beam splitter (PBS) or 50-50% output port as an output of the oscillator. The spectral width is measured as 9 nm centered at 1034 nm with 3.6 ps pulse duration from output port of coupler. Fig 3.3 shows the spectrum and pulse duration of oscillator from the output port of coupler. Average output power is 1.2 mW and pulse energy is 12 pJ. From PBS port, average output power is measured 47 mW. The output of the oscillator is taken from the 50% port of the coupler and it is

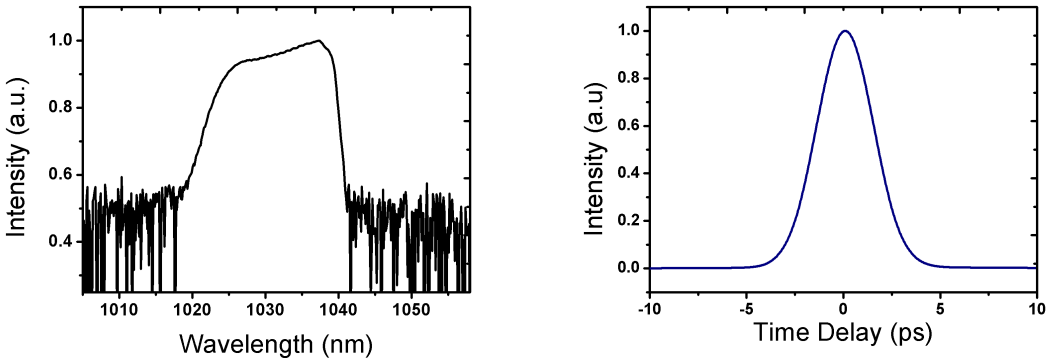

Figure 3.3: (a) Output spectrum of oscillator in linear scale and log scale (inset). (b) 3.6 ps pulse duration which is measured from 50/50 % coupler port of oscillator with intensity autocorrelator.

used as a seed for first amplifier stage. Direct fiber coupling the seed pulses to the amplifier completely eliminates the possibility of interruption of the seed due to misalignment or accidental blocking of the beam.

3.1.2 First Amplifier Stage

After the generating the low power pulses from an oscillator, we need to amplify them for high power levels. This part is the first amplifying stage and pulses which are launched from oscillator are used as a seed . Fig 3.4 shows the schematic of the first amplifier part. The essential performance aspects of fiber amplifiers is modeled by using simulation software. It is possible to quantify various effects on the amplifier performance, and use such results for optimizing the fiber parameters. The optimum length of Yb-doped gain fiber is found as 85 cm with 6/125 μm core/cladding diameter. In this part, the system is also pumped with single mode diode at 976 nm wavelength. We used 1030 nm wavelength light which is coming from oscillator as a seed signal. For combining pump light at 976 nm and signal light at 1030 nm wavelength, wavelength-division multiplexer (WDM) is used. We focus on forward pumping configuration which has an advantages over

the backward pumping configuration especially high power levels. Heat generation is lover than backward pumping because signal and pump powers become maximum at the opposite side of the fiber. Disadvantage of forward pumping is remaining the unabsorbed pump light at the fiber tip.

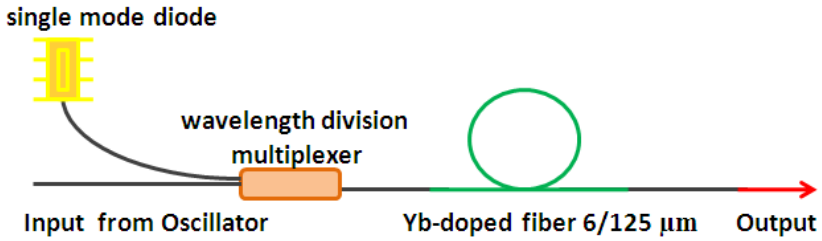

Figure 3.4: Schematic of first amplifier part.

Characterization of the obtained average output power with respect to the applied current of the single mode pump diode and the output spectrum of the first amplifier are shown in Fig 3.5. As seen on the Fig 3.5 when the current level of the single mode pump diode is reached at 600 mA level average output power of the system becomes 102 mW.The spectrum bandwidth of the first stage amplifier is measured as 9.4 nm which is 1.6 nm more than the bandwith of oscillator part.

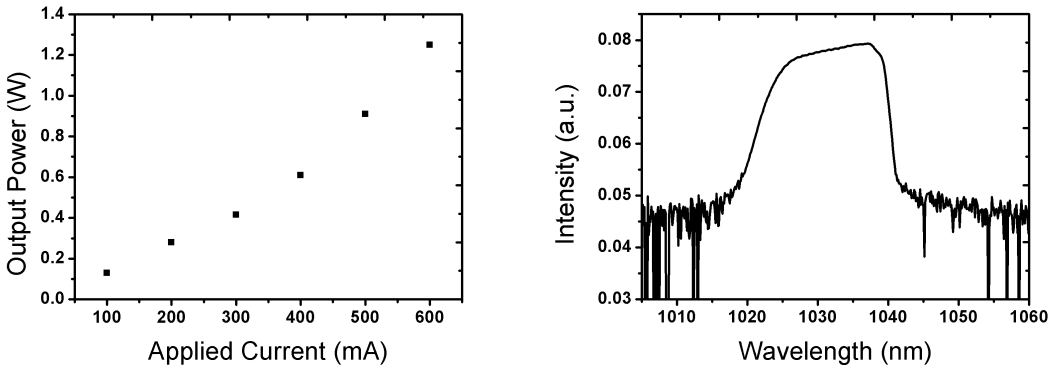

Figure 3.5: (a)First amplifier power graphic with respect to applied current. (b)Spectrum of first amplifier output in log scale.

3.1.3 Gratings Compressor

Laser ablation is categorized by two different regimes which are distinguished by the comparison of the laser pulse duration with the characteristic time of electron-phonon interaction in metal. When the laser pulse duration is shorter than this characteristic time which is corresponds to a few picoseconds, ablation rate is increased. In addition to, pulse duration affects heat dissipation into the sample and ablation quality. Recently, reported experimental results showing that when pulse duration is less than 5 ps, an increase of ablation rate could happen with decreasing the pulse duration with much improved precision and surface quality [47]. For this system, measured pulse duration is 13 ps from output of high power amplifier part without compression of pulses which is not enough for ablation operation.

Chirped pulse amplification (CPA) method is the most common one for compressing the pulses without nonlinear effects at high power and high energy operations. In a CPA ultra-short laser, pulse is stretched out in time for decreasing peak power during amplification and nonlinear effects are reduced by decreasing peak power. When the desired power level is reached, compressor part is placed at the end of system for compressing pulse width. After amplification of pulse energies, amplified pulse is recompressed back to the original pulse width.

Stretching and compressing process is related to group velocity dispersion (GVD). If initial pulse is un-chirped than broadening of the pulse does not depend on the sign of GVD parameter β_2. Therefore, the pulse would broaden same amount for given same dispersion length for both normal and anomalous dispersion regimes. In the case of linearly chirped pulses, the broadening amount depends on the sign of chirp parameter. When the chirp parameter is bigger than zero it is called positive chirp and otherwise negative chirp. If we have positive chirp gaussian pulse in positive dispersion media then pulse is broadened and it is called streching the pulse. On the other hand, if we have positive chirp gaussian pulse in negative dispersion media then pulse is compressed.

We have positive chirp pulses which are obtained from the oscillator. HI1060

fiber from the Corning company is used as passive single mode fiber in the system and HI1060 is positive dispersive media at 1 μm. It could be used as stretcher for pulses and after amplification we can use reflection or transmission gratings for negative dispersion media for compression. Efficiency of compression part is almost 40 % percentages which means that we would get compressed pulse with 40 W average output power if 100 W is launched into the compressor. This system is limited by pump power and we can not increase output power more than 100 W. However material processing requires high average output power and less than 10 ps pulse duration for ablation threshold, so we need to find another method for pulse compression.

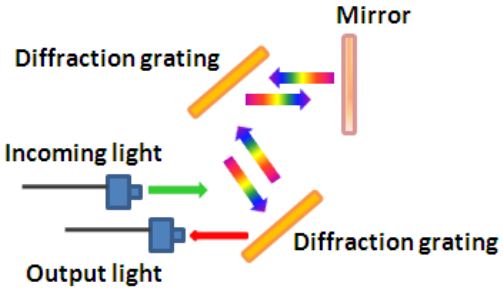

Figure 3.6: Schematics of gratings part.

We placed gratings between first amplifier and second amplifier. Positive chirped pulses are amplified in first stage amplifier up to 102 mW average output power and after that they are inserted into gratings part. Fig 3.6 shows the schematic of the gratings part.In this part two pieces gratings are used. Also, two pieces of collimator are used for sending the pulses through the gratings and collecting pulses after compressing. The purpose of gratings in this system is separating the frequencies of incoming light. After separation of frequencies, high frequency components of pulses have to propagate a longer distance than low-frequency components which means that negative dispersion media is created. By placing the gratings after the first stage amplifier, output gratings shift to negative chirp according to the distance between gratings and negatively chirped pulses can be launched into the last two stages of amplification. When negatively

chirped pulses interact with positive dispersion media they experience spectral narrowing instead of spectral broadening.

Pulses are being collected after grating compressor by collimator and sending through the second stage amplifier. Incoming light has 100 mW average power at the beginning and at the end of this part average power reduces to 30 mW because of the efficiency of gratings. Efficiency of grating system is around 60% and also coupling the light into the collimator causes some losses. A pair of gratings with 900 lines/mm and GVD parameter as -0.0047 ps^2/mm are placed after first amplifier for managing total dispersion by varying the distance. The distance between grating changed from 4 cm to 16 cm corresponds to -0.188 ps^2 to -0.752 ps^2 respectively. By changing the distance between gratings few ps pulse duration is measured as minimum pulse duration at 100 W average output power and it is limited by excessive nonlinear phase shift.

3.1.4 Second Amplifier Stage

First stage amplifier and second stage amplifier have almost same configuration. Forward pumping configuration is preferred for both of them. The difference between two stages are the power levels and components which are used in systems.

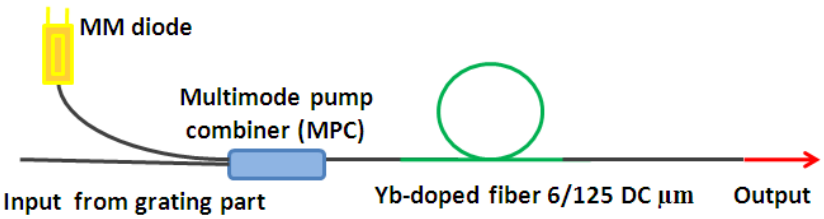

Figure 3.7: Schematics of second amplifier part.

We used multimode pump combiner (MPC) is used instead of WDM because we connected 10 W multimode pump diode from the IPG company into the system for obtaining high power and WDM can not handle such power levels and fibers of WDM are single mode fibers which is different fiber from 10 W

multimode pump diode. Pump wavelength is around 976 nm. For the second stage amplifier 3 meters Yb-doped gain fiber is used. This fiber is Yb-6/125 μm DC fiber instead of single clad fiber. Fig 3.7 shows the schematic of the second stage amplifier.

We used the output of the gratings as a seed for the second stage amplifier. The input signal is around 30 mW. As seen on the table 3.1 at 7.7 A obtained output power is 1.5 W for 1030 nm signal wavelength. 7.7 A is the optimum current which pump diode gives exactly 976 nm wavelength light.

Current (A)	Pump Power (W)	Amplified Signal Power (W)
2	1.12	0.130
3	1.82	0.28
4	2.61	0.415
5	3.3	0.61
6	4.02	0.910
7	4.75	1.25
8	5.51	1.90

Table 3.1: Output power table for second stage amplifier with respect to applied pump diode current.

3.1.5 Power Amplifier Stage

High power amplifier part is the most challenging part of the system. Nonlinear effects and thermal effects start to dominate the system and they limits the power levels. Therefore, we designed high power amplifier part based on those limitations. First, we changed the fiber type to large core DC fiber whose core and cladding diameters are 25/250 μm. Nonlinear effects depend on the peak intensity inside of the fiber and threshold of nonlinear effects is reduced by decreasing the peak intensity with the increasing core diameter. Large-mode area fibers can guide several higher order transverse modes and this affects the beam quality of fiber amplifier. Discrimination of higher order transverse modes and achieving stable fundamental mode operation of fiber amplifier are also other concerns in high power fiber laser systems.

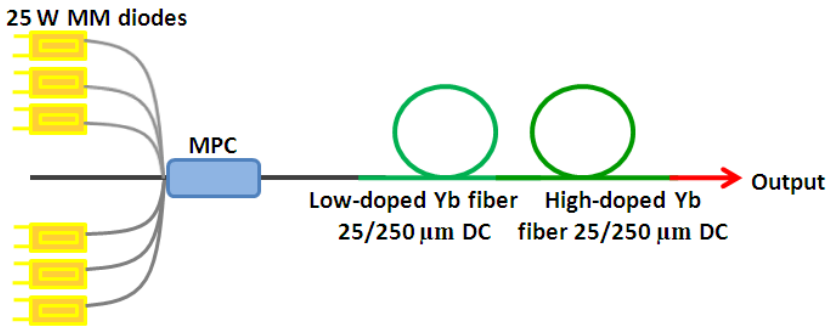

Figure 3.8: Schematics of high power amplifier part.

High power pump diodes are used for high power amplifier which is seen at Fig 2.1. Output power of those diodes approximately 24 W which are bought from Oclaro company and we used six pieces pump diodes in this system. With the combination of pump light and signal light which is coming from second stage amplifier at 1.5W power level by MPC, we obtained 100 W output power at the end of the system. Fig 3.8 shows the schematic of the high power amplifier part. Multimode pump combiner (MPC) is used for combining seed signal and pump light. Input fiber of MPC is 25/250 μm DC fiber and output fiber of MPC is 25/250 μm DC. MPC combines 6 pump ports and 1 signal port.

In this system, we used two different kinds of Yb-doped fiber as a gain medium which are Yb700 25/250 μm and Yb1200 μm which is called hybrid fiber. These two different types of fiberes have different doping concentrations. Fig 3.9 shows heat generation and dissipation through the active fiber (red-dotted line) for high and low doping concentration case and also for hybrid fiber case. High doping concentration fiber generates more heat energy than low doping concentration fiber. To lower the operating temperature in fibers a basic solution is decreasing pump absorption which is used low doping concentration fiber and using a longer fiber length. However, laser suffers from relatively low efficiency and high non-linear effects. As a better solution, arrangement of pump absorption coefficients along the amplifier may improve the laser efficiency and reduce system temperature and nonlinear effects. Therefore, hybrid fiber is used for high power amplifier part. We reduce the temperature of fiber by using low doping concentration at

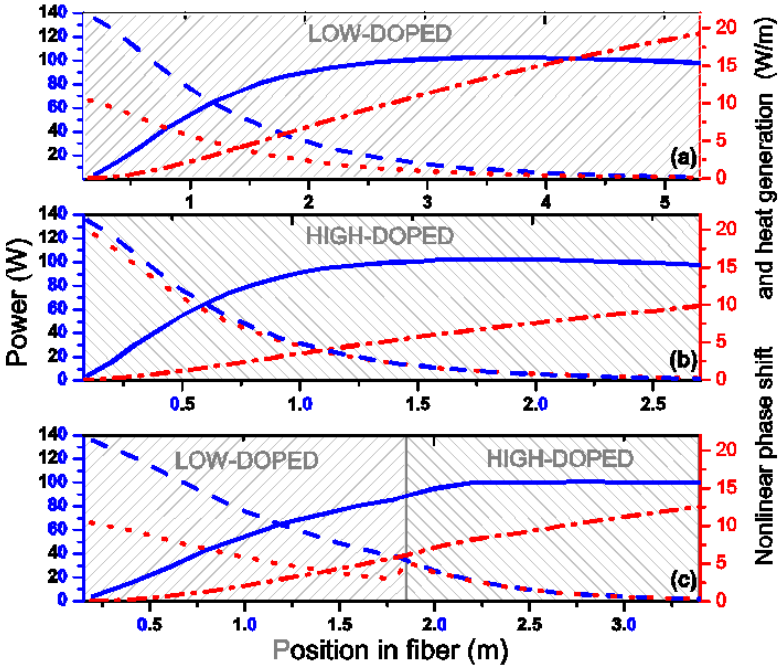

Figure 3.9: (Color online) Simulated evolution of signal (solid curve) and pump (dashed curve) power, nonlinear phase shift (dot-dashed curve) and heat generation per unit length (dotted curve) along (a) low-doped, (b) high-doped, (c) low- and high-doped, hybrid gain fibers [20].

beginning of amplification. After 1.8 meters, we spliced high doped concentration fiber to the system and total active fiber length became 4 meters.

The average power of the high power amplifier is measured and Fig 3.10 shows a graph of output power versus pump power. At 100 W power level system works with 72 % efficiency and spectrum variation is shown for different power levels

The minimum pulse width generated by the simulation is almost 4 ps and could achieve when grating separation is 9.57 mm corresponds to the zero total GVD. Experimentally we obtained 4.1 ps as to minimize pulse width corresponds to 250 kW peak power at full operation when the grating separation is almost 12 mm and the total GVD is almost - $0.12ps^2$. Fig 3.11 shows the intensity autocorrelation and retrieved pulse using the PICASO algorithm based on the

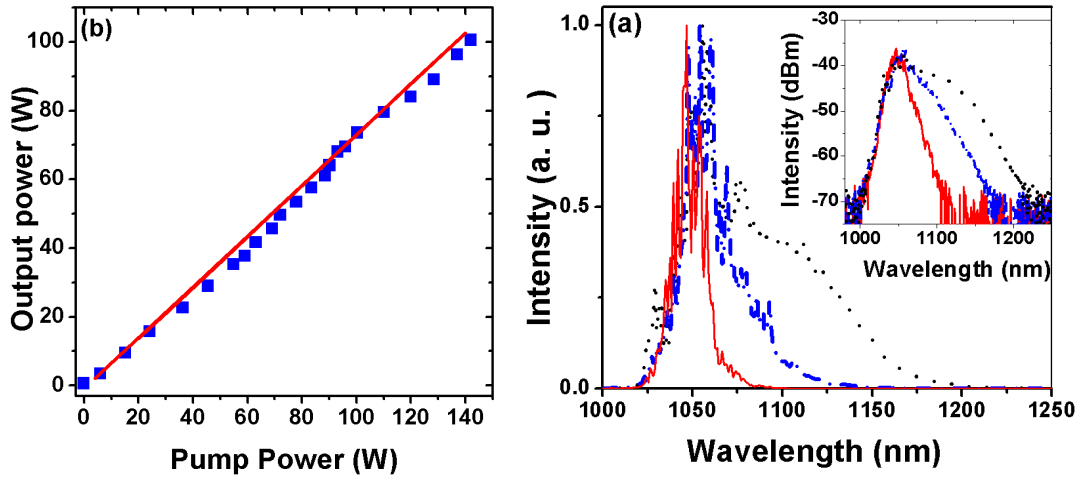

Figure 3.10: (a)Measured output power with respect to launched pump power (b)Spectrum of high power amplifier output (red line (solid) for 50W, blue line (dot-dashed) for 70W and black line (dashed) for 100 W). Inset of the graph is in logarithmic scale [20].

experimental autocorrelation and spectrum measurements. Fig 3.11 shows the behaviour of output pulse width obtained by simulation (red dot curve). A numerical approach employed to study the behaviour of the pulse width versus total GVD. The simulation modelled with generalized nonlinear Schrodinger equation [48].

M^2 is the dimensionless number and it indicates the beam quality of laser systems. The most ideal laser beam is LP_{01} which is the closest to a simple gaussian profile and by definition M^2 is equal to 1 for LP_{01} mode. This is the definition for the diffraction limited beam. Experimentally it is impossible to obtain 1 for value of M^2 because laser beam does not contain only gaussian profile beam. Unabsorbed pump light and other higher order modes can affect the beam quality. Multimode fibers which we are using high power amplifier part can support just a few guided modes which affect the beam quality and brightness of the laser beam. Fig 3.12 shows the M^2 of the system with respect to signal power for both cooling system on and cooling system off.

The search for higher speed processing of material has motivated a wide range of research efforts to scale up average power without sacrificing beam quality.

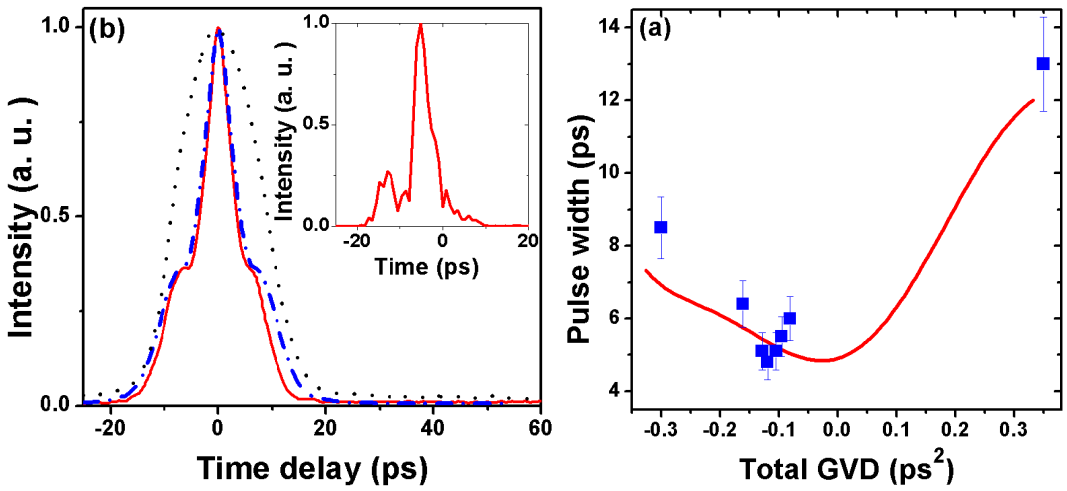

Figure 3.11: (a) Output of the Yb fiber laser at 100 W. Blue curve is the measured intensity autocorrelation and red (dash-dot) is the retrieved pulse by PICASO. Inset graph is the real pulse shape (b) Simulated (solid line-red) and measured pulsewidth [20].

Higher speed processing requires high repetition rate and high average power for ultra-short pulsed lasers. We developed 100 W output power fiber laser system with a 100 MHz repetition rate with and M^2 measurement gives an idea of beam quality. Several groups have used various levels of suppression of higher order modes by adjusting fiber index and dopand distribution, cavity configurations or launch conditions of the beam [49, 50, 51]

For suppression of higher modes, wrapping the gain fiber around a cylindrical mandrel ,whose radius is chosen to provide low loss for the fundamental mode and high loss for other modes, is the most common technique. Higher order modes in the fiber core is somehow extending beyond the core of the fiber. Therefore, we can obtain diffraction limited beam quality by coiling the fiber to induce substantial bend loss for all transverse modes except fundamental mode. However, wrapping the gain fiber causes losses some part of the pump light during the amplification process because of bending radius and this situation affects the efficiency of the system. Therefore, we added one meter 25/250 μm single clad passive fiber at the end of a Yb fiber and wrapped it around cylindrical mandrel

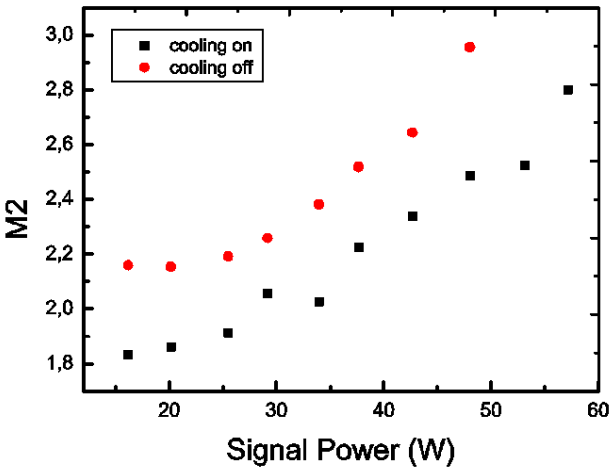

Figure 3.12: M^2 measurement of the system with respect to various output power.

with $D = 6$ cm. With this method, we provided high loss for unabsorbed pump light which propagates in the first cladding and also higher order modes except fundamental mode.

We can suppress the higher order modes by adjusting the seed launch conditions. Coiling the input fiber of amplifier composes bend loss for the higher order modes which generate in the second stage amplifier. Input fiber of high power amplifier part is the output fiber of second amplifier part and input fiber of high power amplifier's MPC. We have a fragile splice joint at that connection. Therefore, we coiled both fibers separately with $D = 6$ cm and then we splice them. The idea for coiling the input fiber of the second stage amplifier is that launching single mode beam into the power amplifier because higher order modes which come from the second stage amplifier can be amplified in that stage. Amplified higher order modes reduces the efficiency of average power of fundamental mode and disrupt the beam quality. Therefore, it affects the efficiency of material ablation operation. Fig 3.12 shows the M^2 measurement of power amplifier with respect to signal power for both cooling systems on and off situation.

3.2 Challenges

3.2.1 Thermal Problems

One of the main problems which are encountered at high power levels is the thermal problems. With the over heating, physical specifications of fibers can be changed and also this heating can disrupt the beam quality of light. Additionally, because of excessive heat generation, some components of the system can be damaged. We encountered the thermal effects on high power laser system with heating at the splice points and on the doped fiber caused by quantum defects. Although highly efficient the quantum defect associated with the lasing of Yb-ions results in around 20% of the pump radiation being converted into heat of the host material [34]. Consequently, optical absorption properties of the coating material along the fiber need to extract waste heat energy from silica host results in heating of the polymer coating. However, coating material has low thermal stability ans it is advisible to keep the operating temperature of the system below 80^o C. Consequently, the coating material limits the output power of fiber laser system or amount of heat should be extracted from the laser system. Yb-doped fiber ends can reach around 400^o C without any active cooling systems [52]. Therefore scaling of high output power levels requires some kind of active cooling.

Thermal management of splices is more difficult than active fibers. Fig 3.13 shows the splice points of the amplifier during operation with an IR camera. As seen on the figure, splice points are brighter than other parts. This indicates that light escapes from those splice points. Especially, as the pump light launches, the temperature peaks at the splice point between MPC and gain fiber, because the gain fiber has the strongest pump absorption. The splice operation induces a non-guided pump or signal power loss and causes a rise in temperature. Therefore, we observe bright spots in Fig 3.13 which indicates the non-guided light. To minimize splice heating, which is critical for reliability of fiber laser systems, we improved splice quality and used active cooling system.

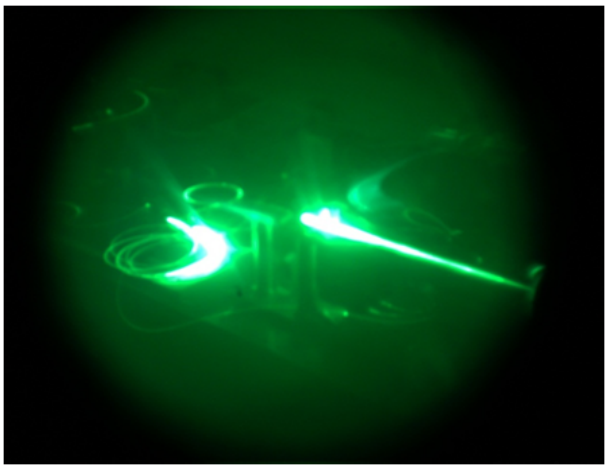

Figure 3.13: Image of system with IR camera during operation. Bright parts are the splice points of the system and thermal effects are effective at that points.

In this system, most common burning problem is the splice point between MPC and Yb fiber at high power amplifier part same as continuous wave 200 W fiber laser system. Therefore, this part also needs special treatment for cooling. We used a same cooling system with 200W CW laser system for the high power amplifier part which is shown in Fig 2.8. We separated that splice point from total gain fiber and hold it on air. Also, we put air fan on top of that splice point for dissipiating excessive heat on that splice point. We do not recoat that splice because the coating material has low thermal stability and constitutes the limiting factor for heat load in the fiber. Fig 3.14 shows the cooling system for amplifier part. In the first image, there is a 20 cm metal plate. First 20 cm of gain fiber is on that plate and there are two peltiers and fans under that plate for cooling plate and fiber. First 20 cm generates more heat energy than rest of gain fiber, because most of the pump conversion appears in this part. Hence, we separate that part of the gain fiber from total gain fiber which is placed on the aluminum plate that has holes. For this system we put a peltier on top of MPC because of too much power loading on the MPC. Also, we can easily fix the temperature of MPC under room temperature.

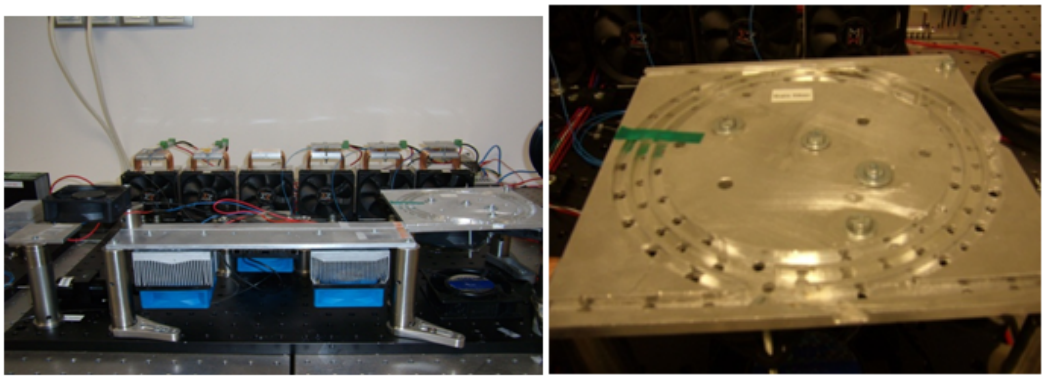

Figure 3.14: (a) Cooling system of high power amplifier part. (b) Alliminium plate with holes and air fans are connected top of that plate for supporting air fan on fibers.

3.2.2 Splices

Splice between single mode and multi mode fibers can be done but they are rare. When single mode fiber is the launching fiber and the multimode fiber is the receiving fiber, then splice loss will be quite low. Fusion splicer covers a range of different geometrical parameters for core diameter, mode field diameter and cladding diameter. Automatic and manuel operation modes are available for the fusion splicer. In our case, manuel operation mode was preffered. First, we decrease the arc power until only melts the surface of the fiber and stick them together which is called cold splice. Larger diameter fibers requires more heat to achieve splicing temperature than smaller diameter fibers. The temperature distribution between two such fibers can be made more equitable by making heat source closer to the large diameter fiber which means that we can give offset to electrodes of splicer through large diameter fiber.

Input fiber of MPC is 25/250 μm and output fiber of second stage amplifier is 6/125 μm. We need to connect these two system with splicing operation. A commercial Vytran type fusion splicer was employed to splice single mode and multimode fiber. Fig 3.15 shows splice image of that point.

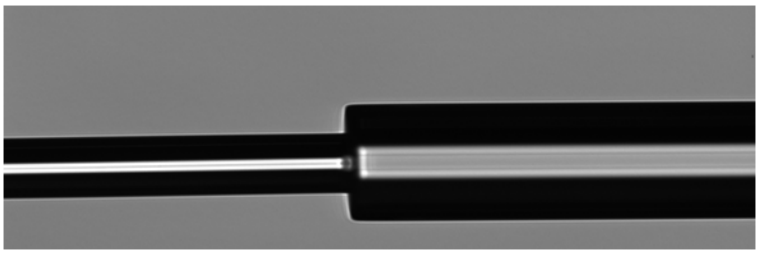

Figure 3.15: Splice image of small diameter fiber and large diameter fiber.

Low loss splice is possible if the light is passing from small diameter to large diameter because energy from single mode fiber will be scattered amongst the many guided modes of multi mode fiber [37].We arrange electrodes position of the splicer and make them closer to the large diameter fiber. After that we need to arrange splice parameters. We use transmitted power technique for understanding splice quality. Therefore, we connect a light source to small diameter fiber and measure the power from the end of that fiber. Then we splice small diameter fiber to large diameter fiber and measure transmitted power from end of large diameter fiber. We can change arc power, arc time and hot push parameters.

3.2.3 Nonlinear Effects

Essential part of applifiying ultra-short pulses is the control of nonlinear effects in the fiber core. The avoidance of nonlinear effects in fiber is the main challenge for power scaling for ultrashort pulse amplification. The fiber based system is able to produce pulse with a peak power 250 kW at 100 W average output power [20]. Pulse energies of up to 1 μm has been demonstrated at 100 MHz repetition rate.

Self-phase modulation creates intensity dependent nonlinear phase during the amplification process. When the pulse duration is short and the peak power is high, the laser field acquires a nonlinear phase shift. B-integral specifies the accumulated nonlinear phase which is produced by peak intensity along the fiber length [53];

$$B \equiv \frac{2\pi}{\lambda} \int_0^L n_2 I(z) dz \tag{3.2}$$

where $I(z)$ is the peak intensity and n_2 is the nonlinear index. For high intensity, value of B integral can become larger than 1. If, the value of B integral is above 3-5, there is a risk for self-focusing which beam collapses to very small radius so that optical intensities are strongly increased and exceed damage threshold. Therefore, with single pulse in this regime, active medium or system component may be damaged. Other effects of self-phase modulation are strong spectral broadening, reduction in the achievable gain and reduced beam quality. This effect depends on the total effective fiber length as shown in equation 3.2 . Fig 3.9 shows the changes of nonlinear phase shift with respect to fiber length. In high power amplification process we need to use fiber both passive and active as short as possible. One of the main reasons for using hybrid fiber is minimizing the B integral. In Fig 3.9 red (dash-dotted) line represent the nonlinear phase shift along the fiber and it indicates accumulated nonlinear phase shift for three configurations with low doped fiber, with high doped fiber and with combination of low doped and high doped fibers.

For intense fields, stimulated Raman scattering can occur in which stokes wave can grow rapidly inside the medium after exceeding the threshold value. A threshold value of SRS depends on the optical intensity of light inside the fiber core and effective length. Reducing the effective fiber length and increasing the fiber core diameter decrease the threshold value of SRS.

3.3 Summary

We have demonstrated a Yb-doped fiber laser amplifier with 4.1 picosecond pulse duration, 100 W of average power and 100 MHz repetition rate. This system is seeded by a passively mode-locked fiber oscillator in the all-normal dispersion regime. Amplifier parts contain three parts and all of them are fiber integrated. Also, this system contains gratings which allows to manage the pulse duration

by changing the gratings separation. Without grating parts, 13 ps pulse duration is obtained at 100 W power level but with gratings we reached approximately 4 ps pulse duration. This system is one of the highest power all-fiber laser systems. Beam quality can be improved by coiling the fiber tighter. The all-fiber integrated design improves stability and allows for direct beam delivery to sample via fiber. In addition, high repetition rate supports higher speed material processing. As such we expect this system to find wide use in experimental and industrial applications.

Chapter 4

Conclusion

Fiber lasers are commonly used in diverse areas including material processing, medical, metrology. Solid-state lasers are the most common laser system because of their excellent beam quality, power scalability, high efficiency. On the other hand fiber lasers are also special types of solid state lasers and they have shown very good progress in recent years. Fiber lasers' application areas are also increasing proportional to their output powers. Fiber lasers have some advantages on other types of lasers such as flexibilities, misalignment free operation, stability, high efficiency and diffraction limited beam quality. In this thesis, we present our work on high-power all-fiber-laser designs and possible application areas of these lasers like material processing.

In chapter 1, general information about the fiber lasers and amplifiers are explained. Amplification of pulses is explained briefly. In the amplification process, possible effects can be encountered like nonlinear effects which are discussed in this chapter. This thesis contains high power fiber laser systems. Therefore, components which are used in high power lasers are also explained in this chapter. All-fiber laser design requires special components and treatments especially in high power applications. Despite, the high power fiber laser component splice points have also significant importance.

Chapter 2, contains the all-fiber integrated continuous wave high power laser systems. This system is all-fiber integrated and it works at 1060 nm wavelength. The output power of this laser system is limited by only pump power and the quality of both components and splice points. Also, thermal management has importance. Therefore, we built an air cooling system based on over-heating parts of the system which are splice points and gain fiber part. Also, we developed a simulation software which models the laser as a modified two-level system which can be found in the appendix A. With this simulation optimized system parameters can be calculated and the system can be modified in a good way based on the results of the simulations.

Chapter 3 describes a high-power ultrashort pulsed laser system. This system produces pulses with few picosecond pulse duration and the repetition rate is 100 MHz. The average output power of this laser is 100 W which is one of the highest average power lasers for all-fiber integrated amplifier part in the world. 100 MHz repetition rate is chosen for the material processing applications. This system is used for material processing applications in high speed regime now. This laser contains oscillator part which pulses are produced and after that three part amplifiers which are used for amplifying the average power of the laser. For controlling the pulse duration after the first amplifier part, there is a grating part and this part give negative dispersion to pulses. With this method, the minimum system pulse duration is measured as $\sim$5-ps. We have initiated experiments where we use this laser system for high-speed material processing. These results will be discussed elsewhere. The parameters of this laser system were chosen to achieve optimal, high-speed ablation of metal targers. A few-ps pulse duration is enough for obtaining non-thermal material ablation process. 100 MHz is for speeding up the operation. High repetition rate requires high average power for obtaining high pulse energy for ablation threshold, so we need to increase average power. Material processing with high speed and high average power is an unknown area and we believe that we will obtain good results such as high precision even if small interaction areas with high speed process. Therefore, we are developing this system by increasing the average power and repetition rate.

Bibliography

[1] T.H.Maiman, "Stimulated optical radiation in ruby," *Nature*, vol. 4736, no. 187, pp. 493–494, 1960.

[2] R.G.Gould, "The laser, light amplification by stimulated emission of radiation," *The Ann Arbor Conference on Optical Pumping, The University of Michigan*, vol. 28, no. 7, p. 128, 1959.

[3] A.D.Colley H.J.Baker, "Planar waveguide, 1 kW CW, Carbon Dioxide Laser Excited by a Single Transverse RF Discharge," *Applied Physics Letters*, vol. 61, no. 2, 1959.

[4] C.Steven, M.Larionoy and A.Giesen, "Yb:YAG thin disk laser with 1 kW output power," *Optical Society of America*, pp. 35–41, 2000.

[5] E.Stiles, "New developments in IPG fiber laser technology," *5 th International Workshop on Fiber Lasers*, 2009.

[6] J. L. Baird, "British patent 285,738," 1928.

[7] A. C. S. Van Heel, "A new method of transporting optical images without aberration," *Nature*, vol. 173, no. 39, 1954.

[8] C. K. Kao and G. A. Hockham, "Dielectric-fibre surface waveguides for optical frequencies.," *Proc. IEE*, vol. 113, no. 7, 1966.

[9] R. H. Stolen, E. P. Ippen and A. R. Tynes, "Raman oscillation in glass optical waveguide," *Applied Physics Letters*, vol. 20, no. 62, 1972.

[10] E. P. Ippen and R. H. Stolen, "Stimulated Brillouin scattering in optical fibers," *Applied Physics Letters*, vol. 21, no. 539, 1972.

[11] A. Hasegawa and F. Tappert, "Transmission of stationary nonlinear optical pulses in dispersive dielectric fibers," *Applied Physics Letters*, vol. 23, no. 142, 1973.

[12] L. F. Mollenauer, R. H. Stolen and J. P. Gordon, "Experimental observation of picosecond pulse narrowing and solitons in optical fibers," *Phys. Rev. Lett.*, vol. 45, no. 1095, 1980.

[13] V. Fomin,M. Abramov,A. Ferin,A. Abramov,D. Mochalov,N. Platonov and V. Gapontsev, "10 kW single mode fiber laser," *Proc. of 5 th International Symposium on high-Power Fiber Lasers and Their Applications, St Petersburg, Russia*, 2010.

[14] B. E. A. Saleh, "Fundamentals of Photonics," *Wiley, New York*, 1991.

[15] R.J. Mears and L.Reekie, "Low-noise erbium-doped fiber amplifier operating at 1.54 nm," *Electron Letter*, vol. 23, pp. 1026–1028, 1987.

[16] Y. Jeong and J.K.Sahu, "Ytterbium-doped Large-core fiber laser with 1.36 kW continuous wave output power.," *Optics Express*, vol. 12, pp. 6088–6092, 2004.

[17] J. Y.Jeong, "Ytterbium-doped large core fiber laser with 1 kW continuous wave output power.," *Advanced Solid State Photonics, Sante Fe, New York.*, 2004.

[18] D.Gapontsev and N.Platonov., "2 kW CW ytterbium fiber laser with record diffraction-limited brightness," *Conference on Lasers and Electro-Optics Europe*, 2005.

[19] U. W. K. Albers, "Optical pump concepts for highly efficient quasi-three-level lasers," *Applied Physics B*, vol. 105, no. 2, pp. 245–254, 2011.

[20] P. Elahi S. Yilmaz Ö. Akçaalan H. Kalaycoğlu, B. Öktem,Ç. Şenel, F. Ö. İlday, and K. Eken., "Doping management for high-power fiber lasers: 100

W, few-picosecond pulse generation from an all fiber integrated amplifier," *Optics Letters*, vol. 37, no. 15, 2012.

[21] K. Ozgoren, "83 W 3.1 MHz square-shaped 1-ns pulsed all-fiber-integrated laser for micromachining," *Optics Express*, vol. 19, no. 18, pp. 17647–17652, 2011.

[22] D. J. Nilsson and W. A. Clarkson, "High power fiber lasers: current status and future perpectives," *J. Opt. Soc. Am. B*, vol. 27, no. 11, 2010.

[23] Y. Xiao, F. Brunet, M. Kanskar, M. Faucher, A. Wetter, and N. Holehouse, "1-kilowatt CW all-fiber laser oscillator pumped with wavelength-beam combined diode stacks," *Optics Express*, vol. 20, no. 3, pp. 3296–3301, 2012.

[24] T. Eidam, S. Hanf, E. Seise, T. V. Andersen, T. G. Christian Wirth, T. Schreiber, J. Limpert and A. Tunnermann, "Femtosecond fiber CPA system emitting 830 W average output power," *Optics Letters*, vol. 35, no. 94, 2010.

[25] R. S. Chen, W. Yang and Q. Lu, "157 W all-fiber high power picosecond laser," *Applied Optics*, vol. 51, no. 13, pp. 2497–2500, 2012.

[26] C.J.Koester and E.Snitzer, "Amplification in a fiber laser," *Applied Optics*, vol. 3, no. 1182, 1964.

[27] R.J.Mears, L.Reekie, S.B. Poole, D.Payne, "Low threshold CW and Q-switched fiber laser operating at 1.55 μm," *Electron Letters*, vol. 22, no. 159, 1986.

[28] Luis Zenteno, "High-power Double-clad fiber lasers," *journal of lightwave technology*, vol. 11, no. 9, 1993.

[29] V. P. Gapontsev, "Penetration of fiber lasers into industrial market," *Proc. SPIE 6873, Fiber Lasers V: Technology, Systems, and Applications*, 2008.

[30] F. Stutzki, F. Jansen, A. Liem, C, Jaurequi, J. Limpert and A. Tunnermann, "26 mJ 130 W Q-switched fiber laser system with near diffraction limited beam quality," *Optics Letters*, vol. 37, no. 6, pp. 1073–1075, 2012.

[31] M.Wickham, E.C.Cheung, J.G. Ho, M.Weber, "Coherent combination of fiberlasers with a diffractive optical element," *Advanced Solid State Photon., OSA Tech. Dig. Ser., Japan*, 2008.

[32] Y.Shamir, Y.Sintov, M.Shtaif, "Incoherent beam combining of multiple single mode fiber lasers utilizing fused tapered bundling," *Proc. SPIE 7580*, 2010.

[33] H. M. and J. L. Rogers, "Self organized coherence in fiber laser arrays," *Optics Letters*, vol. 30, no. 11, pp. 1339–1341, 2005.

[34] J. Limpert, F. Röser, T. Schreiber, and A. Tünnerman, "High-Power Ultrafast Fiber Laser Systems," *Journal of Selected Topics in Quantum Electronics*, vol. 12, no. 2, 2006.

[35] J. Limpert, A. Liem, H. Zellmer, and A. Tunnermann, "500 W continuous wave fibre laser with excellent beam quality," *Optics Express*, vol. 11, no. 7, p. 818, 2003.

[36] Y.Wang, C.Xu and H.Po, "Thermal effects in kilowatt fiber lasers," *Photonics Technology Letters*, vol. 16, no. 1, 2004.

[37] A.D.Yablon, "Optical Fusion Splicing," *Springer-Verlag Heidelberg*, 2005.

[38] H.Injeyan and G.D.Goodno, "High Power Laser Handbook," *McGraw-Hill*, 2011.

[39] N. S. Platonov, D. V. Gapontsev, V. P. Gapontsev, and V. Shumilin, "135 W cw fiber laser with perfect single mode output," *Proc. Conf. Lasers Electro-Optics, Long Beach, CA, post-deadline paper CPDC3.*, 2002.

[40] A. Yusim, J. Barsalou, D. Gapontsev, N. S. Platonov, O. Shkurikhin, V. P. Gapontsev, Y. A. Barannikov, F. V. Shcherbina, "100 watt single-mode CW lineraly polarized all-fiber format 1.56 μm laser with suppression of parasitic lasing effects," *Proc. SPIE 5709, Fiber Laser || : Technology, Systems and Applications, 69*, 2005.

[41] S. Yin, P. Yan, and M. Gong , "End-pumped 300 W continuous wave ytterbium-doped all-fiber laser with master oscillator multi-stage power amplifiers configuration.," *Optics Express*, vol. 16, no. 22, 2008.

[42] R. Paschotta, J. Nilsson, A. C. Tropper, and D. C. Hanna, "Ytterbium-Doped Fiber Amplifiers," *IEEE Journal of Quantum Electronics*, vol. 33, no. 7, 1997.

[43] R. Paschotta, "Field Guide to Optical Fiber Technology," *SPIE field Guides Volume FG16, Bellingham, Washington USA*, 2009.

[44] Y. Jeong, J.K. Sahu, R.B. Williams, D.J. Richardson, K. Furusawa and J. Nilsson., "Ytterbium-doped large core fibre laser with 272W output power," *Electronics Letters*, vol. 39, no. 13, 2003.

[45] X. Liu, D. Du, and G. Mourou., "Laser Ablation and Micromachining with Ultrashort Laser Pulses," *journal of Quantum Electronics*, vol. 33, no. 10, 1997.

[46] F. Roser, T. Eidam, J. Rothhard, O. Schmidth, N. Schimpf, J. Limpert and A. Tunnermann., "Millijoule pulse energy high repetition rate femtosecond fiber chirped pulse amplification system," *Optics Letters*, vol. 32, no. 3495, 2007.

[47] J. Yang, Y. Zhao, N. Zhang, Y. Liang, and M. Wang, "Ablation of metallic targets by high-intensity ultrashort laser pulses," *Physical Review B*, vol. 7, 2007.

[48] P.K.Mukhopadhyay, K.Özgoren, İ. L. Budunolu and F. Ö. İlday, "All-fiber low noise high power femtosecond Yb-fiber amplifier system seeded by an all-normal dispersion fiber oscillator.," *IEEE J. Sel. Topics Quantum Electron*, vol. 15, no. 1, 2009.

[49] H. L. Offerhaus, N. G. Broderick, D. J. Richardson, R. Sammut, J. Caplen and L. Dong , "High energy single transverse mode Q-switched fiber laser based on a multimode large mode area erbium-doped fiber.," *Optics Letters*, vol. 23, 1998.

[50] J. M. Sousa and O. G. Okhotnikov, "Multimode Er-doped fiber for single transverse-mode amplification," *Applied Physics Letters*, vol. 74, no. 11, 1999.

[51] M. E. Fermann, "Single mode excitation of multimode fibers with ultrashort pulses," *Optics Letters*, vol. 23, no. 52, 1998.

[52] A. Carter, B. Samson, K. Tankala, D. P. Machewirt, V. Khitrov, U. H. Manyam, F. Gonthier, and F. Seguin, "Damage Mechanisms in Components for Fibre Lasers and Amlifiers," *Laser-Induced Damage in Optical Materials, SPIE, Bellingham, WA*, 2004.

[53] G. P. Agrawal, "Nonlinear Fiber Optics," *San Diego, CA, USA Elseiver Inc*, 2007.

Appendix A

Gain Dynamics

For the simulation of realistic high power laser systems the Lorentzian gain model is not sufficient. Therefore a new model was developed which uses the original absorption and emission cross-section of Yb in the gain fiber. In this model, rate equations were used for calculating the upper and ground state population [42]:

$$\frac{dn_2}{dt} = (R_{12} + W_{12})n_1 - (R_{21} + W_{21} + A_{21})n_2 \tag{A.1}$$

$$\frac{dn_1}{dt} = -(R_{12} + W_{12})n_1 + (R_{21} + W_{21} + A_{21})n_2, \tag{A.2}$$

where R_{12} and R_{21} are the lower-to-upper and upper-to-lower transition rates for the pump, respectively; W_{12} and W_{21} are the lower-to-upper and upper-to-lower transition rates, respectively for the signal. A_{21} is the spontaneous emission rate, which is equal to $1/\tau$. Equations 1 and 2 give the steady-state values of upper and ground state population, n_1 and n_2, as;

$$n_2 = \frac{R_{12} + W_{12}}{R_{12} + R_{21} + W_{12} + W_{21} + A_{21}} \tag{A.3}$$

$$n_1 = 1 - n_2 \tag{A.4}$$

The transition rates for the pump are given by $R_{12} = \frac{\sigma_{12}^{(p)} P_p}{h\nu_p A_p}$ and $R_{21} = \frac{\sigma_{21}^{(p)} P_p}{h\nu_p A_p}$. The transition rates for the signal are given by $W_{12} = \frac{\sigma_{12}^{(s)} P_s}{h\nu_s A_s}$ and $W_{21} = \frac{\sigma_{21}^{(s)} P_s}{h\nu_s A_s}$. Here, $\sigma_{12}^{(s)}$ and $\sigma_{21}^{(s)}$ are the effective signal absorption and emission cross-sections, respectively. Likewise, $\sigma_{12}^{(p)}$ and $\sigma_{21}^{(p)}$ are the effective pump absorption and emission

cross-sections, respectively. A_p and A_s are the effective modal areas for pump and signal, respectively.

$$\frac{dP_p}{dz} = \eta_p(\sigma_{21}^{(p)} n_2 - \sigma_{12}^{(p)} n_1) N_{tot} P_p \tag{A.5}$$

$$\frac{dP_s^i}{dz} = \eta_{si}(\sigma_{21}^{(s_i)} n_2 - \sigma_{12}^{(s_i)} n_1) N_{tot} P_s^i, \tag{A.6}$$

where $P_{s(p)}^i$ is the signal (pump) power at frequency ν_i. Equation 7 and 8 gives the gain and loss for the pump and signal at a longitudinal position z. N_{tot} is the total density of the Yb ions in m^{-3}. η_s and η_p are the overlap factors between the light-field modes and Yb ions distribution. However, we extend the gain model of [42] to incorporate a range of frequencies for the signal as well as forward and backward amplified spontaneous emission (ASE) power. Pump is assumed to be monochromatic. Hence, the generalized rate equations can be written as:

$$n_2 = \frac{\sum \frac{\sigma_{12}^{(p)}}{A_p h\nu_p} P_p + \frac{\sigma_{12}^{(s_i)}}{A_{eff,s} h\nu_i} P_s^i + \frac{\sigma_{12}^{(a_i)}}{A_s h\nu_j} P_a^i}{\sum \frac{\sigma_{12}^{(p)} + \sigma_{21}^{(p)}}{A_p h\nu_p} P_p + \frac{\sigma_{12}^{(s_i)} + \sigma_{21}^{(s_i)}}{A_s h\nu_i} P_s^i + \frac{\sigma_{12}^{(a_i)} + \sigma_{21}^{(a_i)}}{A_s h\nu_i} P_a^i + \frac{1}{\tau}}, \tag{A.7}$$

where $n_1 = 1 - n_2$. ASE power for frequency, P_a^i, contains forward traveling ASE component $P_a^{+,i}$ and backward traveling ASE component $P_a^{-,i}$.

$$P_a^i = P_a^{+,i} + P_a^{-,i} \tag{A.8}$$

The new field propagation equations can be written in terms of field powers with the possible intrinsic background loss in the fiber such as α_p, $\alpha_{\nu i}$, $\alpha_{\nu j}$:

$$\frac{dP_p}{dz} = \eta_p(\sigma_{21}^{(p)} n_2 - \sigma_{12}^{(p)} n_1) N_{tot} P_p - \alpha_p P_p \tag{A.9}$$

$$\frac{dP_s^i}{dz} = \eta_s(\sigma_{21}^{(si)} n_2 - \sigma_{12}^{(si)} n_1) N_{tot} P_s^i - \alpha_{\nu_i} P_s^i \tag{A.10}$$

$$\frac{dP_a^{+,i}}{dz} = \eta_a(\sigma_{21}^{(aj)} n_2 - \sigma_{12}^{(aj)} n_1) N_{tot} P_a^{+,i} + \eta_a \sigma_{21}^{(aj)} n_2 N_{tot} h\nu_j \delta\nu_j - \alpha_{\nu_j} P_a^{+,i} \tag{A.11}$$

$$\frac{dP_a^{-,i}}{dz} = -\eta_a(\sigma_{21}^{(aj)} n_2 - \sigma_{12}^{(aj)} n_1) N_{tot} P_a^{-,i} - \eta_a \sigma_{21}^{(aj)} n_2 N_{tot} h\nu_j \delta\nu_j + \alpha_{\nu_j} P_a^{-,i} \tag{A.12}$$

These equations require two boundary conditions at $z = 0$ and $z = L$ with L is the length of the gain fiber. This formulation requires bidirectional split-step method for the calculation of pump, signal and forward and backward ASE.

Appendix B

Code

```
clear;clc
%-------------------------------------------------------------------------
%General parameters
%-------------------------------------------------------------------------
tic;
c = 3e8; %Speed of light in [m/s]
h = 6.626e-34; %Planck constant in [J.s]

%-------------------------------------------------------------------------
%Flags for fiber type and pump direction
%-------------------------------------------------------------------------
gain_fiber_type = 0; % "Yb =0 ; Er = 1"

%-------------------------------------------------------------------------
%Pump parameters
%-------------------------------------------------------------------------
lambda_p = 975e-9;   %Pump wavelength in [m]
P_p = 300; %0.27  %Pump power in [W]
del_lam_p = 1e-10;   % pump spectrum resolution ".1nm fixed"
pump_bw = 5e-9; % pump bandwidth "by user"
```

```
%-------------------------------------------------------------------------
%Fiber parameters
%-------------------------------------------------------------------------
L = 7.5; %Length in [m]
d_core = 25e-6; %Core diameter in [m]
mfd_pump = 250e-6; %Mode-field diameter for pump in [m]
mfd_signal = 19.7e-6; %Mode-field diameter for signal in [m]
alpha_s = 0.0; % signal loss [m^-1]
alpha_p = 0.0; %pump loss [m^-1]
eta = 0.91; %efficiency coefficient
%Ntot = 4.8e25;% density of Yb+ ions per cubic meter [parts/m^3]
Ntot = 5e25; %9e25/2.;
% [ref. Opt. Lett. 33(19), 2221-2223]

%-------------------------------------------------------------------------
%Simulation parameters
%-------------------------------------------------------------------------
step = 2000; %Total number of steps
% tres = 4096; %Total number of data points
% t0 = 100; %Number of data points corresponds to FWHM
round_max = 10; %Maximum number of iterations
Dmin = 1e-3; %Maximum fraction error
%-------------------------------------------------------------------------
%Fiber Bragg Grating
%-------------------------------------------------------------------------
fbg1=0.99;
fbg2=0.07;
%-------------------------------------------------------------------------
%Plotting options
%-------------------------------------------------------------------------
% plot_input = 0; %Make it 1 to plot the input signal spectrum
% plot_output = 0; %Make it 1 to plot the output signal spectrum
```

```
plot_power = 1; %Make it 1 to plot the power distribution in fiber
plot_forwASE = 0; %Make it 1 to plot the forward ASE spectrum
plot_backASE = 0; %Make it 1 to plot the backward ASE spectrum
plot_pump_in =0; %Make it 1 to plot the input pump spectrum
plot_pump_out =0; %Make it 1 to plot the input pump spectrum
plot_forward =1; %Make it 1 to plot the forward signal spectrum
plot_backward =1; %Make it 1 to plot the backward signal spectrum
%-------------------------------------------------------------------------
%Pump Spectrum creation
%-------------------------------------------------------------------------
l = 10*pump_bw/del_lam_p;
lam_p = (-l/2:l/2)*del_lam_p/1.667;
spect_p = exp(-(lam_p).^2/pump_bw^2*1.667^2);
spect_p = spect_p.*P_p/ sum(spect_p)/del_lam_p.*del_lam_p;
lam_p = lam_p+lambda_p;

%-------------------------------------------------------------------------
%Loading  fiber absoption and emmision specturm file
%-------------------------------------------------------------------------
if (gain_fiber_type == 0)
    load yb_m.mat;

    ind_max = 290;
    ind_min = 151;
    t1 = 0.85e-3; %upper state life time in [s]
    del_lam = 1.25e-10; % delta lambda for ASE
    lam_ase = xlam(ind_min):del_lam:xlam(ind_max);
    s12_ase = spline(xlam',ya',lam_ase);
            % Absorption spectra coeff. for ASE (new wavelengths axis)
    s21_ase = spline(xlam',ye',lam_ase);
            % Emmision spectra coeff. for ASE (new wavelengths axis)
    arr_len = length(lam_ase);
    % FBG reflection profile
```

```
    lam_fbg = lam_ase(1,471:491);
    fbg_fwhm = .3e-9%.1274e-9;
    len_fbg = length(lam_fbg);
    fbg_gauss = exp(-(lam_fbg-lam_fbg(1,(len_fbg+1)/2)).^2/(fbg_fwhm/1.667)^2);


elseif (gain_fiber_type == 1)
    load Er_m.mat;
    ind_max = 1200;
    ind_min =102;
    xlam = lam;
    ya = ea;
    ye = ee;
    t1 = 10e-3; %upper state life time in [s]
    lam_ase(1:1099) = lam(102:1200); % wavelength axis for ASE
    del_lam = 2e-10;                 % delta lambda for ASE
    s12_ase(1:1099) = ea(102:1200);
    % Absorption spectra coeff. for ASE (new wavelengths axis)
    s21_ase(1:1099) = ee(102:1200);
    % Emmision spectra coeff. for ASE (new wavelengths axis)
    arr_len = 1099;
    clear lam ea ee
else
    printf('Error: Incorrect fiber type')
    exit;
end

%-------------------------------------------------------------------------
%s12_s and s21_s creation
%-------------------------------------------------------------------------
s12_p = spline(xlam,ya,lam_p);
s21_p = spline(xlam,ye,lam_p);
P0_ase = h*c^2*del_lam./lam_ase.^3;
```

```
%
%-------------------------------------------------------------------------
% Parameters for cavity signals
%-------------------------------------------------------------------------
s12_s(1:len_fbg)= s12_ase(471:491);
s21_s(1:len_fbg)= s21_ase(471:491);
lam_s(1:len_fbg)= lam_ase(471:491);

%-------------------------------------------------------------------------
%Propagation
%-------------------------------------------------------------------------
% Defining boundry values for Pump, Signal, Forward and Backword ASE
Pparr = zeros(step+1,length(lam_p));
Pparr(1,:) = spect_p;
SF_arr = zeros(step+1,len_fbg);
SB_arr = zeros(step+1,len_fbg);
PaseFwd_arr = zeros(step+1,arr_len);
PaseFwd_arr(1,:) = P0_ase;
PaseBwd_arr = zeros(step+1,arr_len);
PaseBwd_arr(step+1,:) = P0_ase;
a_core = pi*((d_core/2.0)^2);
a_clad = pi*((mfd_pump/2.0)^2);
a_signal = pi*((mfd_signal/2.0)^2);
PaseFwd_prv = PaseFwd_arr;
PaseBwd_prv = PaseBwd_arr;
W12 = 0;
W21 = 0;
%-------------------------------------------------------------------------
%Round trip calculations
%-------------------------------------------------------------------------

for round = 1:round_max % Alternate iterations in forward and backword direction
```

```
SF_arr(1,:) = fbg1*fbg_gauss.*(SB_arr(1,:)+PaseBwd_arr(1,471:491));
PaseBwd_arr(1,471:491)=0.01.*PaseBwd_arr(1,471:491);
for n = 1:step
    R12 = sum(s12_p.*(Pparr(n,:)./(a_clad)).*lam_p./c./h);
    R21 = sum(s21_p.*(Pparr(n,:)./(a_clad)).*lam_p./c./h);
    A21 = 1/t1;
    W12 = sum(s12_s.*(SF_arr(n,:)+SB_arr(n,:))./a_signal.*lam_s./c./h);
    W21 = sum(s21_s.*(SF_arr(n,:)+SB_arr(n,:))./a_signal.*lam_s./c./h);
    P12 = sum(s12_ase.*(PaseFwd_arr(n,:)+PaseBwd_arr(n,:))
               ./a_signal.*lam_ase./c./h);
    P21 = sum(s21_ase.*(PaseFwd_arr(n,:)+PaseBwd_arr(n,:))
                ./a_signal.*lam_ase./c./h);

    n2 = (R12+W12+P12)/(R12+R21+W12+W21+P12+P21+A21);
    n1 = 1-n2;

    Pparr(n+1,:) = Pparr(n,:).*(1+a_core/a_clad*(s21_p.*n2-s12_p.*n1)
                  .*Ntot*L/step).*exp(-alpha_p*L/step);
    SF_arr(n+1,:) = SF_arr(n,:).*(1+((d_core/mfd_signal)^2)
                   *(eta*s21_s.*n2-s12_s.*n1).*Ntot.*L./step)
                   .*exp(-alpha_s*L/step);
    PaseFwd_arr(n+1,:) = PaseFwd_arr(n,:).*(1+((d_core/mfd_signal)^2)
                   *(eta*s21_ase*n2-s12_ase*n1).*Ntot.*L./step)
                   .*exp(-alpha_s*L/step)+s21_ase.*n2.*Ntot.*P0_ase.*L./step
                   .*exp(-alpha_s*L/step);
end
% Loop for backward propagaing ASE

SB_arr(step+1,:) = fbg2*fbg_gauss.*(SF_arr(step+1,:)
                  +PaseFwd_arr(step+1,471:491));
PaseFwd_arr(step+1,471:491)=0.93.*PaseFwd_arr(step+1,471:491);
for n = step+1:-1:2
    R12 = sum(s12_p.*(Pparr(n,:)./(a_clad)).*lam_p./c./h);
```

```
    R21 = sum(s21_p.*(Pparr(n,:)./(a_clad)).*lam_p./c./h);
    A21 = 1/t1;
    W12 = sum(s12_s.*(SF_arr(n,:)+SB_arr(n,:))./a_signal.*lam_s./c./h);
    W21 = sum(s21_s.*(SF_arr(n,:)+SB_arr(n,:))./a_signal.*lam_s./c./h);
    P12 = sum(s12_ase.*(PaseFwd_arr(n,:)+PaseBwd_arr(n,:))
          ./a_signal.*lam_ase./c./h);
    P21 = sum(s21_ase.*(PaseFwd_arr(n,:)+PaseBwd_arr(n,:))./a_signal
          .*lam_ase./c./h);

    n2 = (R12+W12+P12)/(R12+R21+W12+W21+P12+P21+A21);
    n1 = 1-n2;
    SB_arr(n-1,:) = SB_arr(n,:).*(1+((d_core/mfd_signal)^2)
                    *(eta*s21_s.*n2-s12_s.*n1).*Ntot.*L./step)
                    .*exp(-alpha_s*L/step);
    PaseBwd_arr(n-1,:) = PaseBwd_arr(n,:).*(1+((d_core/mfd_signal)^2)
                         *(eta*s21_ase*n2-s12_ase*n1).*Ntot.*L./step)
                         .*exp(-alpha_s*L/step)+s21_ase
                         .*n2.*Ntot.*P0_ase.*L./step.*exp(-alpha_s*L/step);
end

% Loop termination condition
% (del(PaseFwd)+del(PaseBwd))/(PaseFwd+PaseBwd)<Dmin
disp(round)
if round~=1
    D = (sum(sum(abs(PaseFwd_arr-PaseFwd_prv)))
      +sum(sum(abs(PaseBwd_arr-PaseBwd_prv))))
      /(sum(sum(abs(PaseFwd_arr)))+sum(sum(abs(PaseBwd_arr))));
    disp(D);
    if D<Dmin; break; end
end

PaseFwd_prv = PaseFwd_arr;
PaseBwd_prv = PaseBwd_arr;
```

```
end
PaseFwd_arr;
PaseBwd_arr;

PaseFws = PaseFwd_arr(step+1,:);
PaseBws = PaseBwd_arr(1,:);
Pplast = Pparr(step+1,:);
SFwd = SF_arr(step+1,:);
SBwd = SB_arr(1,:);


%-------------------------------------------------------------------------
%Ploting
%-------------------------------------------------------------------------
if plot_pump_in==1
    figure;
    plot(lam_p,spect_p./del_lam_p);
    axis tight;
    %     xlim([(lambda_s-50e-9) (lambda_s+100e-9)]);
    ylabel('Input Pump Spectrum [W/m]');
    xlabel ('Wavelength [m]');
    grid on;
end
if plot_pump_out==1
    figure;
    plot(lam_p,Pplast./del_lam_p);
    axis tight;
    %     xlim([(lambda_s-50e-9) (lambda_s+100e-9)]);
    ylabel('Output Pump Spectrum [W/m]');
    xlabel ('Wavelength [m]');
    grid on;
end
if plot_forwASE==1
```

```
    figure;
    plot(lam_ase,PaseFws);
    axis tight;
    %     xlim([(lambda_s-50e-9) (lambda_s+100e-9)]);
    ylabel('Output Forward ASE Spectrum [W/m]');
    xlabel ('Wavelength [m]');
    grid on;
end
if plot_backASE==1
    figure;
    plot(lam_ase, PaseBws);
    axis tight;
    %     xlim([(lambda_s-50e-9) (lambda_s+100e-9)]);
    ylabel('Backward ASE Spectrum [W/m]');
    xlabel ('Wavelength [m]');
    grid on;
end

if (plot_power==1)% &&(pump_direction ==0)
    figure;
    fiber = 0:L/step:L;
    PaseFwd_arr = PaseFwd_arr';
    PaseBwd_arr = PaseBwd_arr';
    Pparr = Pparr';
    plot(fiber,sum(PaseFwd_arr),'r',fiber,sum(PaseBwd_arr),'b',
          fiber,sum(Pparr),'g', fiber,sum(SF_arr'),
          'k',fiber,sum(SB_arr'),'m'); % ,fiber,sum(Psarr),'black'
    xlabel('Position [m]');
    ylabel('Forward ASE(Red), Backward ASE(Blue) and
       Pump(Green) Power[W]');% Signal(Black),
    grid on;
    axis tight;
end
```

```
if plot_forward ==1
figure;
plot(lam_s, SFwd);
grid on
end
if plot_backward ==1
figure;
plot(lam_s, SBwd);
grid on
end
toc;
```